

Kernel-Based Distributed Q-Learning: A Scalable Reinforcement Learning Approach for Dynamic Treatment Regimes

Di Wang^a, Yao Wang^a, Shaojie Tang,^b Shao-Bo Lin^{a*}

^a Center for Intelligent Decision-Making and Machine Learning, School of Management, Xi'an Jiaotong University, Xi'an, China

^b Naveen Jindal School of Management, University of Texas at Dallas, Richardson, Texas, USA

In recent years, large amounts of electronic health records (EHRs) concerning chronic diseases, such as cancer, diabetes, and mental disease, have been collected to facilitate medical diagnosis. Modeling the dynamic properties of EHRs related to chronic diseases can be efficiently done using dynamic treatment regimes (DTRs), which are a set of sequential decision rules. While Reinforcement learning (RL) is a widely used method for creating DTRs, there is ongoing research in developing RL algorithms that can effectively handle large amounts of data. In this paper, we present a novel approach, a distributed Q-learning algorithm, for generating DTRs. The novelties of our research are as follows: 1) From a methodological perspective, we present a novel and scalable approach for generating DTRs by combining distributed learning with Q-learning. The proposed approach is specifically designed to handle large amounts of data and effectively generate DTRs. 2) From a theoretical standpoint, we provide generalization error bounds for the proposed distributed Q-learning algorithm, which are derived within the framework of statistical learning theory. These bounds quantify the relationships between sample size, prediction accuracy, and computational burden, providing insights into the performance of the algorithm. 3) From an applied perspective, we demonstrate the effectiveness of our proposed distributed Q-learning algorithm for DTRs by applying it to clinical cancer treatments. The results show that our algorithm outperforms both traditional linear Q-learning and commonly used deep Q-learning in terms of both prediction accuracy and computation cost.

Key words: Q-learning, dynamic treatment regimes, distributed learning, kernel ridge regression

* Corresponding authors: sblin1983@gmail.com

1. Introduction

Patients with chronic diseases, such as cancer, diabetes, and mental disease, normally undergo a long period of initial treatment, disease recurrence, and salvage treatment. Explicitly specifying the relationship of treatment type and drug dosage with patient response is generally difficult, so practitioners have to use protocols in which each patient receives a similar treatment based on the average responses of previous patients with similar cases. However, illnesses respond heterogeneously to treatment. For example, a study on schizophrenia (Ishigooka et al. 2000) discovered that patients using the exact same antipsychotic experience drastically varied outcomes; some patients experience few adverse events with improved clinical outcomes, whereas others have to discontinue treatment due to worsening symptoms. This has motivated researchers to advocate dynamic treatment regimes (DTRs) to determine treatments dynamically and individually based on clinical observations of patients (Murphy 2005a, Lavori and Dawson 2008, Chakraborty and Moodie 2013, Chakraborty and Murphy 2014, Almirall and Chronis-Tuscano 2016).

A DTR is defined by a set of sequential decision rules; each rule takes the clinical observations of a patient at certain key points as input and returns the treatment action of doctors as output (Tsiatis et al. 2019). In this way, the design of a DTR can be considered a sequential decision-making problem and suits the reinforcement learning (RL) framework (Sutton and Barto 2018), in which states, actions, rewards, and policies correspond to the clinical observations of patients, treatment options, treatment outcomes, and series of decision rules, respectively. RL addresses sequential decision-making problems with sampled, evaluative, and delayed feedback simultaneously, which naturally makes it a desirable tool for developing ideal DTRs.

Q-learning (Watkins and Dayan 1992) is a typical temporal-difference algorithm that produces a sequence of high-quality actions in RL and has substantially developed in the past decades in health care (Yu et al. 2021, Oh et al. 2022), control (Moore et al. 2011, 2014), recommendation (Zhao et al. 2017, Yoganarasimhan 2020), and other management-related problems (Peters and Schaal 2008, Kalashnikov et al. 2018, Schultz and Sokolov 2018). In particular, Padmanabhan et al. (2017)

used different reward functions in Q-learning to model different constraints in cancer treatments. In contrast to other application areas (Gosavi 2009), Q-learning for modern DTRs typically has the following important characteristics:

- **Data structure:** Due to the fact that treatment decisions are often made at specific intervals, it is not possible to generate a treatment history of infinite duration. When a patient’s chronic disease is not effectively treated or managed through a particular treatment plan, they may seek alternative treatment options from other doctors, resulting in treatment records with limited duration. Additionally, in Q-learning for DTRs, doctors typically have a limited number of treatment options to choose from based on patients’ treatment histories (Tsiatis et al. 2019, Chap.1.4). However, for a given treatment decision, the clinical observations of patients can be unpredictable, resulting in an infinite number of states. This makes Q-learning for DTRs distinct from classical tabular-based Q-learning, which focuses on finite actions and states (Gosavi 2009). To summarize, DTRs have finite horizons, and each stage of Q-learning for DTRs has a finite number of actions but an infinite number of states.

- **Task orientation:** Unlike other applications of Q-learning (Gosavi 2009), the treatment decisions made at each key point in Q-learning for DTRs play a crucial role in determining patients’ health outcomes, regardless of when these decisions are made. For example, a poor treatment decision at some stage may lead to severe negative consequences that cannot be corrected by subsequent treatments. As a result, it is not appropriate to assume that the treatment at one point is more important than others, and the common approach of discounting rewards in Q-learning (Even-Dar and Mansour 2003, Liu and Su 2022) is not suitable for DTRs. In short, the reward of Q-learning cannot be discounted for DTRs.

- **Quality guarantee:** Quality is crucial in medical treatment, as even a small mistake can result in negative outcomes for patients. This necessitates not only a strong understanding of the reasons and methods behind specific treatment decisions but also robust and solid theoretical guarantees supporting the effectiveness of Q-learning. This requirement eliminates the use of some heuristic yet intricate designs of Q-learning (Oroojlooyjadid et al. 2022, Fan et al. 2020) for generating DTRs.

- **Computation costs:** In recent years, large amounts of EHRs related to chronic diseases, such as cancer, diabetes, and mental illness, have been collected to aid in medical diagnosis. This increase in data size has allowed for the identification of previously unknown symptoms, but it also poses significant scalability challenges for the Q-learning algorithms used, in terms of storage and computational complexity. As a result, commonly used but computationally intensive approaches, such as deep Q-learning (François-Lavet et al. 2018), are not suitable for DTRs.

The characteristics discussed above place strict limitations on the use of Q-learning for generating DTRs. The need for quality guarantees excludes the commonly used linear Q-learning (Murphy 2005b), and the demands for computational efficiency and interpretability make the widely adopted deep Q-learning (Oroojlooyjadid et al. 2022) unsuitable for DTRs. In this paper, we aim to create a scalable Q-learning algorithm that has solid theoretical guarantees for DTRs.

1.1. Mathematical formulation of Q-learning for DTRs

DTRs often involve T -stage treatment decision problems. Let $s_t \in \mathcal{S}_t$ be the pretreatment information and $a_t \in \mathcal{A}_t$ be the treatment decision at stage t , where \mathcal{S}_t and \mathcal{A}_t are sets of pretreatment information and treatment decisions, respectively. A history of personalized treatment is generated in the form of $\mathcal{T}_T = \{s_{1:T+1}, a_{1:T}\}$, where s_{T+1} is the status after all treatment decisions are made and $s_{1:T} = \{s_1, \dots, s_T\}$. Let $R_t : (\mathcal{S}_{1:t+1}, \mathcal{A}_{1:t}) \rightarrow \mathbb{R}$ be the clinical outcome following the decision a_t , which depends on the pretreatment information $s_{1:t+1}$ and treatment history $a_{1:t}$. A suitable function R_t should be identified to quantify the outcome in DTRs because R_t encodes the professional knowledge of doctors and defines the value of their treatment decisions. In cancer treatment, for example, R_t can be set as the tumor size or the estimated survival time when the t -th treatment decision is made. Our purpose is not to search for appropriate clinical outcome functions R_t but to develop an efficient learning scheme for generating a high-quality DTR for a given R_t . Throughout the paper, we use capital letters (A_1, A_2 , etc.) to denote random variables and lowercase letters (a_1, a_2 , etc.) to represent their realization.

A DTR $\pi = (\pi_1, \dots, \pi_T)$, where $\pi_t : \mathcal{S}_t \times \mathcal{A}_{t-1} \rightarrow \mathcal{A}_t$, is a set of rules for personalized treatment decisions at all T stages. The optimal DTR is that which maximizes the overall outcome of interest

$\sum_{t=1}^T R_t(s_{1:t+1}, a_{1:t})$ in terms of designing suitable treatment rules $\pi = (\pi_1, \dots, \pi_T)$. Our analysis is cast in a random setting to quantify the overall outcome (Murphy 2005b, Sugiyama 2015). Denote by $\rho_t(s_t | s_{1:t-1}, a_{1:t-1})$ the transition probability of s_t conditioned on $s_{1:t-1}$ and $a_{1:t-1}$. The value of DTR π at stage t is then defined by

$$V_{\pi,t}(s_{1:t}, a_{1:t-1}) = E_{\pi} \left[\sum_{j=t}^T R_j(S_{1:j+1}, A_{1:j}) \middle| S_{1:t} = s_{1:t}, A_{1:t-1} = a_{1:t-1} \right],$$

where E_{π} is the expectation with respect to the distribution

$$P_{\pi} = \rho_1(s_1) \mathbf{1}_{a_1 = \pi_1(s_1)} \prod_{t=2}^T \rho_t(s_t | s_{1:t-1}, a_{1:t-1}) \mathbf{1}_{a_t = \pi(s_{1:t}, a_{1:t-1})} \rho_{T+1}(s_{T+1} | s_{1:T}, a_{1:T}),$$

and $\mathbf{1}_W$ is the indicator of the event W . Denote the optimal value function of π at stage t as

$$V_t^*(s_{1:t}, a_{1:t-1}) = \max_{\pi \in \Pi} V_{\pi,t}(s_{1:t}, a_{1:t-1}),$$

where Π denotes the collection of all treatments. We aim to find a policy $\hat{\pi}$ to minimize $V_1^*(s_1) - V_{\hat{\pi},1}(s_1)$.

Let $p_t(a_t | s_{1:t}, a_{1:t-1})$ be the probability that a decision a_t is made given the history $\{s_{1:t}, a_{1:t-1}\}$.

Define the optimal time-dependent Q -function by

$$Q_t^*(s_{1:t}, a_{1:t}) = E[R_t(S_{1:t+1}, A_{1:t}) + V_{t+1}^*(S_{1:t+1}, A_{1:t}) | S_{1:t} = s_{1:t}, A_{1:t} = a_{1:t}], \quad (1)$$

where E is the expectation with respect to

$$P = \rho_1(s_1) p_1(a_1 | s_1) \prod_{t=2}^T \rho_t(s_t | s_{1:t-1}, a_{1:t-1}) p_t(a_t | s_{1:t}, a_{1:t-1}) \rho_{T+1}(s_{T+1} | s_{1:T}, a_{1:T}). \quad (2)$$

Given the definition of V_t^* , we derive

$$V_t^*(s_{1:t}, a_{1:t-1}) = V_{\pi^*,t}(s_{1:t}, a_{1:t-1}) = E_{\pi^*} \left[\sum_{j=t}^T R_j(S_{1:j+1}, A_{1:j}) \middle| S_{1:t} = s_{1:t}, A_{1:t-1} = a_{1:t-1} \right],$$

where π^* is the optimal policy. Therefore,

$$V_t^*(s_{1:t}, a_{1:t-1}) = \max_{a_t} Q_t^*(s_{1:t}, a_{1:t}). \quad (3)$$

With (3), the optimal treatment decisions can be determined by maximizing the optimal Q -functions. Thus, researchers have developed efficient algorithms for finding optimal Q -functions, which are named Q -learning algorithms (Watkins and Dayan 1992), in the realm of RL. With $Q_{T+1}^* = 0$, the definition of Q_t^* indicates that

$$Q_t^*(s_{1:t}, a_{1:t}) = E \left[R_t(S_{1:t+1}, A_{1:t}) + \max_{a_{t+1}} Q_{t+1}^*(S_{1:t+1}, A_{1:t}, a_{t+1}) \mid S_{1:t} = s_{1:t}, A_{1:t} = a_{1:t} \right] \quad (4)$$

for $t = T, T-1, \dots, 1$. This property connects Q -functions with the well-known regression function (Györfi et al. 2006) in supervised learning as follows. Denote $\mathcal{X}_t = \mathcal{S}_{1:t} \times \mathcal{A}_{1:t}$ and \mathcal{L}_t^2 as the space of square-integrable functions defined on \mathcal{X}_t with respect to the distribution

$$P_t = \rho_1(s_1) p_1(a_1 | s_1) \prod_{j=2}^t \rho_j(s_j | s_{1:j-1}, a_{1:j-1}) p_j(a_j | s_{1:j}, a_{1:j-1}).$$

Write

$$x_t := \{s_{1:t}, a_{1:t}\} \in \mathcal{X}_t, \quad \text{and} \quad y_t^* := R_t(s_{1:t+1}, a_{1:t}) + \max_{a_{t+1}} Q_{t+1}^*(s_{1:t+1}, a_{1:t}, a_{t+1}). \quad (5)$$

Then, (4) implies that the Q_t^* of each t is the regression function of the input–output pair (x_t, y_t^*) and written as

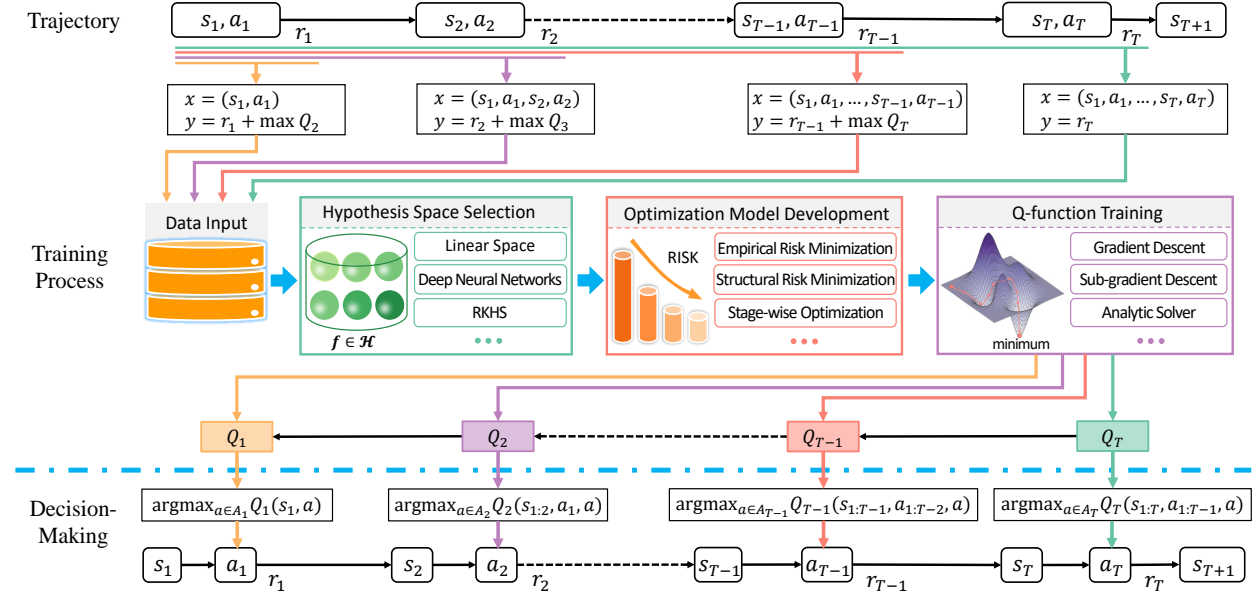
$$Q_t^* = E[Y_t^* | X_t = x_t], \quad t = T, T-1, \dots, 1. \quad (6)$$

Therefore, the standard approach in statistical learning theory (Györfi et al. 2006, Cucker and Zhou 2007) yields

$$Q_t^* = \arg \min_{Q_t \in \mathcal{L}_t^2} E[(Y_t^* - Q_t(X_t))^2], \quad t = T, T-1, \dots, 1, \quad (7)$$

showing that optimal Q -functions can be obtained by solving T least squares problems. In this way, Q -learning for DTRs can be solved as shown in Figure 1.

As shown in Figure 1, through the iterative generation of input–output pairs, Q -learning can be regarded as a series of supervised learning problems and incorporates four steps: hypothesis space selection, optimization model development, Q -function training, and policy search. The hypothesis space selection step focuses on selecting a class of functions that encodes some a priori information

Figure 1 Training and decision-making flows of Q-learning.

and determines the formats of Q-functions. Linear spaces (Murphy 2005b) and deep neural networks (Fan et al. 2020) are typical hypothesis spaces for Q-learning. The optimization model development step involves mathematically defining the Q-functions via a sequence of optimization problems. The empirical risk minimization principle (Murphy 2005a, Sugiyama 2015) is widely used for this purpose. After the optimization model is developed, a feasible optimization algorithm, such as an analytic solver (Murphy 2005b) or a gradient-based algorithm (Sutton and Barto 2018), is designed in the Q-function training step to derive Q-functions. Finally, the policy search step searches for the best possible policies for choosing appropriate actions by maximizing the Q-functions.

1.2. Problem setting

Given the data structure feature of Q-learning for DTRs, we are interested in Q-learning with T stages whose state space \mathcal{S}_t is an infinite continuous space and whose action space \mathcal{A}_t is a discrete set of finite elements. We aim to search for a suitable hypothesis space, develop an appropriate optimization strategy, design an efficient algorithm to train high-quality Q-functions, and derive a DTR with solid theoretical guarantees. To suit different chronic diseases, the proposed Q-learning algorithm for DTRs should be feasible, efficient, and theoretically sound for a large number of reward functions because different reward functions usually correspond to various chronic diseases (Padmanabhan et al. 2017). The setting of Q-learning in this paper is shown in Table 1.

Table 1 Setting of Q-learning for DTRs.

Horizon	Action space	State space	Reward function	Discount	Quality
T	Finite	Continuous	Smooth	No	Generalization error

As the starting point of Q-learning, hypothesis spaces regulate the format and properties of the Q-functions to be learned and determine the type of optimization models to be developed. Therefore, the selection of hypothesis spaces is a constant problem in Q-learning (Sugiyama 2015). In particular, excessively large hypothesis spaces are beneficial for representing any Q-functions but inevitably require large computations, whereas excessively small hypothesis spaces lack expressive power and consequently exclude the optimal Q-functions. Linear spaces (Murphy 2005b) and deep neural networks (François-Lavet et al. 2018) are widely known hypothesis spaces for Q-learning, and they have been used successfully in various applications (Sutton and Barto 2018, Kraus et al. 2020, Oroojlooyjadid et al. 2022). However, linear spaces have limited expressive power and cannot adapt to different reward functions, frequently performing poorly for chronic diseases, such as cancer and sepsis (Yu et al. 2021, Sec.4), whereas deep neural networks lack solid theoretical guarantees and are usually time consuming (training a neural network for specific applications of deep Q-learning requires the tuning of a great number of parameters in nonconvex nonsmooth optimization models); moreover, the running mechanisms of deep Q-learning are difficult to identify. Given the requirement for Q-learning for DTRs to have a balance between having an expressive hypothesis space for quality guarantees and a small and simple hypothesis space for scalability, we are faced with the following challenge:

PROBLEM 1. How can a hypothesis space be designed for Q-learning for DTRs that avoids the limitations of both linear spaces and deep neural networks simultaneously?

Problem 1 is challenging to address because hypothesis spaces with high expressive power are large and require many parameters for training Q-functions, which leads to significant training time, particularly when the data size is large. Once the hypothesis space is determined, optimization models play a crucial role in defining Q-functions. In general, a good optimization model for

Q-learning for DTRs should be solvable, scalable, and interpretable. Solvability means that the developed model can be solved using standard optimization algorithms, such as gradient descent, subgradient descent, and analytic solvers. Scalability implies that the cost of solving the optimization problem is reasonable. Interpretability means that the developed model is easy to understand. Optimization models with good solvability, scalability, and interpretability can be easily developed for linear hypothesis spaces, but for nonlinear spaces, these properties are difficult to achieve. Furthermore, given the limited expressive power of linear spaces, we focus on the following problem:

PROBLEM 2. How can optimization models for Q-learning for DTRs, which are solvable, scalable, and interpretable, be developed to optimize the performance of chosen nonlinear or infinite hypothesis spaces?

The solvability and scalability of optimization models imply that scalable optimization algorithms exist to solve these models, and the finiteness of the treatment options in DTRs means that policy search can be easily implemented. Thus, the solutions to Problems 1 and 2 are sufficient to develop DTRs through Q-learning. With the emphasis on the quality guarantee of Q-learning for DTRs, we ultimately focus on the following problem:

PROBLEM 3. How can the quality of the resulting DTRs be theoretically measured and how can solid theoretical guarantees be provided for it?

Unlike other applications, such as recommendations and supply chain management, which use regret (Liu and Su 2022) to measure the quality of the developed policies, DTRs focus on the final treatment outcomes, regardless of the median treatment processes, in order to fully explore the values of the initial states. This means that new measurement and analysis tools are required for theoretical guarantees.

1.3. Our contributions

We develop a scalable Q-learning algorithm for DTRs to address the above challenges. Our study is driven by three key observations. Based on Problems 1 and 2, a nonlinear or infinite hypothesis space is needed to avoid the limitations of linear spaces, but the optimization model, which is based

on the hypothesis space, should have a linear solution to be solvable, scalable, and interpretable. Kernel methods (Evgeniou et al. 2000), which map data inputs to kernel-based feature spaces to make learning methods linear, have been widely used for regression over the past two decades. The well-known representer theorem (Wahba 1990) states that even though the hypothesis spaces of kernel methods are reproducing kernel Hilbert spaces (RKHS) of infinite dimensions, kernel methods always build estimators in linear spaces whose dimensions are the sizes of the samples. This unique property of kernel methods perfectly meets the requirements of Problems 1 and 2. Additionally, numerous scalable variants of kernel methods, such as distributed learning (Zhang et al. 2015), learning with subsampling (Gittens and Mahoney 2016), and localized support vector machine (SVM) (Meister and Steinwart 2016), have been proposed to reduce the computational burden of kernel methods for regression purposes. Since Q-learning can be regarded as a T -stage least squares regression problem, a scalable Q-learning algorithm can be easily designed based on kernel methods using previously proposed approaches (Zhang et al. 2015, Gittens and Mahoney 2016, Meister and Steinwart 2016).

Based on the above observations, we propose a kernel-based distributed Q-learning algorithm for DTRs. Our main contributions are as follows:

- **Methodological Novelty:** Our approach combines distributed learning (Zhang et al. 2015) and kernel ridge regression (KRR) (Caponnetto and De Vito 2007) to estimate Q-functions, by breaking down Q-learning into T least squares regression problems. Specifically, we use an RKHS corresponding to a kernel as the hypothesis space and implement distributed regularized least squares as the optimization model. This approach avoids the limitations of linear Q-learning while addressing the computational efficiency issues of deep Q-learning. To the best of our knowledge, this is the first attempt to design a distributed Q-learning algorithm with solid theoretical guarantees.
- **Theoretical Novelty:** We propose a novel integral operator approach to analyze the generalization error of Q-learning. Our method allows us to derive tight generalization error bounds for the proposed kernel-based distributed Q-learning algorithm. Our theoretical results indicate that the

distributed operator does not increase the generalization error, given that the data is not divided into too many subsets. Additionally, the generalization error bounds we derived are independent of the input dimensions, indicating that the proposed algorithm scales well with respect to the dimensionality of the problem.

- **Numerical Novelty:** We evaluate the proposed algorithm against linear Q-learning and deep Q-learning in two types (small and large action spaces) of clinical trials for cancer treatments. Our numerical results show that the performance of our approach is consistently better than that of linear Q-learning and no worse than that of deep Q-learning. In terms of computation costs, our approach requires significantly less training time than deep Q-learning. These results demonstrate the effectiveness and efficiency of kernel-based distributed Q-learning for DTRs.

The rest of this paper is organized as follows. Section 2 introduces some related work and compares our approach with theirs. In Section 3, we explain the proposed kernel-based distributed Q-learning algorithm for DTRs. In Section 4, we study the theoretical behaviors of the proposed algorithm by establishing two generalization error bounds, whose proofs are given in the appendix. In Section 5, two simulations concerning clinical cancer treatments are conducted to illustrate how the proposed algorithm outperforms linear Q-learning and deep Q-learning.

2. Related Work and Comparisons

In this section, we compare our approach with some related work on Q-learning for DTRs, theoretical guarantees of Q-learning, and scalable kernel methods.

2.1. Q-learning for DTRs

With the rapid development of medical digitization, EHRs concerning chronic diseases, such as cancer, diabetes, and mental disease, have been collected to facilitate medical diagnosis. EHRs have been widely used in health care decisions regarding chronic diseases over the last decade, including cancer prediction and analysis (Zhao et al. 2011, Humphrey 2017), warfarin dosing (Consortium 2009, Bastani and Bayati 2020), sepsis treatment (Marik et al. 2017, Raghu et al. 2017), and anesthesia analysis (Moore et al. 2011, 2014). Q-learning is a promising approach to utilizing EHRs

to yield high-quality DTRs and has gained fruitful clinical effects in improving the quality of health care decisions (Tsiatis et al. 2019, Yu et al. 2021). Zhao et al. (2009) used support vector regression (SVR) (Vapnik et al. 1996) and extremely randomized trees (Ernst et al. 2005) to fit approximated Q-functions for agent dosage decision-making in chemotherapy; Humphrey (2017) employed classification and regression trees (CART) (Breiman et al. 1984), random forests (Breiman 2001), and a modified version of multivariate adaptive regression splines (Friedman 1991) to estimate Q-values for an advanced generic cancer trial; Tseng et al. (2017) presented a multicomponent deep RL framework for patients with non-small-cell lung cancer (NSCLC) in which a deep Q-network (DQN) maps states into potential dose schemes to optimize future radiotherapy outcomes; Raghu et al. (2017) proposed a fully connected dueling double DQN approach to learn an approximation of the optimal action–value function for sepsis treatment. The reader is referred to Tables III and IV of (Yu et al. 2021) for more related work on Q-learning for DTRs.

Our approach offers three main novelties. First, we employ kernel-based Q-learning to generate DTRs because the design of kernel methods satisfies the high requirements of Q-learning for DTRs (the hypothesis space of a kernel method is large enough, and the derived estimator is in a linear space). Second, we focus on distributed Q-learning algorithms for DTRs that scales well according to the data size. Such a scalable variant of Q-learning for DTRs has not been considered in the literature. Finally, we provide solid theoretical guarantees for the proposed Q-learning approach in the framework of statistical learning theory (Sugiyama 2015), which is beyond the scope of the above mentioned papers.

2.2. Generalization error analysis for Q-learning

Q-learning (Watkins and Dayan 1992) is one of the most commonly employed methods for RL, and it sequentially estimates Q-functions backward (from the last stage to the first stage). Generally speaking, the quality of a Q-learning algorithm is indicated by three factors: generalization performance, computation costs, and stability. The generalization performance depicts the relationship between the number of samples and the value of the derived policy. The computation costs, including the

storage requirements, training time, and testing time, reflect the scalability of Q-learning. Stability describes the relationship between the generalization performance and adopted algorithmic or model parameters, which implies the difficulty of training.

From the statistical learning theory viewpoint, the quality of Q-learning has been studied extensively. In particular, Even-Dar and Mansour (2003) derived a sufficient condition of the learning rate in gradient-based linear Q-learning to guarantee the convergence (stability) of Q-learning; Kearns and Singh (1999), Murphy (2005b), Goldberg and Kosorok (2012), and Oh et al. (2022) studied the generalization error of linear Q-learning; Sabry and Khalifa (2019) and Wainwright (2019) developed several variance reduction techniques to improve the performance of Q-learning; Fan et al. (2020) deduced a generalization error estimate for deep Q-learning; Xu et al. (2005, 2007) and Liu and Su (2022) studied regret bounds for kernel-based Q-learning. However, the setting of Q-learning studied in the current paper is different from those in most of these works, as we are concerned with the states, actions, and rewards in Table 1. For example, except for (Murphy 2005b, Goldberg and Kosorok 2012), and (Oh et al. 2022), all the above studies focused on Q-learning with large (or even infinite) horizons and discount rewards.

The most closely related works to ours are (Oh et al. 2022) and (Liu and Su 2022). The former deduced a similar generalization error to ours for linear Q-learning under the same setting as in the present paper, whereas the latter aimed to derive regret bounds for kernel-based Q-learning. The differences between our work and (Oh et al. 2022) are as follows. We study kernel-based distributed Q-learning rather than linear Q-learning. The main advantage of utilizing an RKHS as the hypothesis space is its excellent expressive power over linear spaces. Moreover, we employ a novel integral operator approach to deduce the generalization error of Q-learning for DTRs rather than use the standard covering number approach. The generalization error bounds in our paper, derived under weaker assumptions on data distribution, are considerably tighter than the results in (Oh et al. 2022). The main differences between our work and (Liu and Su 2022) are three aspects. First, we are interested in generalization error analysis, whereas Liu and Su (2022)

focused on regret analysis. Because the goal of treatment is to find a DTR $\hat{\pi}$ that minimizes $V_1^*(s_1) - V_{\hat{\pi},1}(s_1)$, the generalization error $E[V_1^*(s_1) - V_{\hat{\pi},1}(s_1)]$ is more appropriate for DTRs than the regret $\sum_{t=1}^T ((V_t^*(s_{1:t}, a_{1:t-1}) - V_{\hat{\pi},t}(s_{1:t}, a_{1:t-1})))$. Furthermore, Liu and Su (2022) imposed strong restrictions on the kernel (linear kernel or Gaussian kernel), whereas our approach is available to any positive-definite kernel. Finally, as we use a distributed version of kernel methods, the computation costs of the proposed kernel-based distributed Q-learning approach for DTRs are much less than those of the kernel-based algorithms in (Liu and Su 2022).

2.3. Kernel-based distributed learning for regression

Kernel-based distributed learning is a popular computation reduction strategy for kernel methods in regression. Numerous kernel-based distributed learning algorithms, such as distributed KRR (DKRR) (Zhang et al. 2015, Lin et al. 2017), kernel-based distributed gradient descent (Lin and Zhou 2018), distributed spectral algorithms (Guo et al. 2017, Mücke and Blanchard 2018), and coefficient-based distributed kernel learning (Shi 2019), have been developed with solid theoretical guarantees. Optimal generalization error bounds for DKRR were established in (Lin et al. 2017) in the standard least squares regression framework.

For a specific t , (7) shows that Q-learning can be reduced to least squares regression directly, indicating that our theoretical results can be derived from (Lin et al. 2017) directly. However, there are two main challenges in borrowing the idea of the integral operator approach from (Lin et al. 2017). First, the iterative definition of Q-functions (4) makes it difficult to present a uniform bound of the derived Q-functions, making the approach in (Lin et al. 2017) unavailable for our analysis. As shown in Appendix A.5, a novel iterative method based on operator differences is proposed to bound the uniform bound of Q-functions. Second, we require an additional multistage error to embody the multistage nature of Q-learning, unlike the approaches in (Lin et al. 2017) and (Chang et al. 2017), which divided the generalization error into approximation error to infer the massiveness of the hypothesis space, sample error to describe the model and data quality, and distributed error to quantify the limitation of distributed learning. These challenges hinder the direct use of the results of (Lin et al. 2017) for Q-learning and require delicate analysis and mathematical tools.

3. Kernel-Based Distributed Q-Learning for DTRs

Since (7) is defined by expectation, Q_t^* cannot be derived directly. The only thing we have access to is a set of records of personalized treatments $D := \{\mathcal{T}_{i,T}, r_{i,1:T}\}_{i=1}^{|D|}$, where $\{\mathcal{T}_{i,T}\}_{i=1}^{|D|} = \{(s_{i,1:T+1}, a_{i,1:T})\}_{i=1}^{|D|}$ is assumed to be drawn independently and identically (i.i.d.) according to P , $r_{i,t} := R_t(s_{i,1:t+1}, a_{i,1:t})$, and $|D|$ denotes the cardinality of the set D . We derive an approximation of Q_t^* using D , which is a standard regression problem in supervised learning (Györfi et al. 2006). Empirically, by setting $\hat{Q}_{T+1} = 0$, we can compute Q -functions (\hat{Q}_t for $t = T, T-1, \dots, 1$) by solving the T structural risk minimization problem

$$\hat{Q}_t(s_{1:t}, a_{1:t}) = \arg \min_{Q_t \in \mathcal{H}_t} \mathbb{E}_{|D|} \left[\left(R_t(S_{1:t+1}, A_{1:t}) + \max_{a_{t+1}} \hat{Q}_{t+1}(S_{1:t+1}, A_{1:t}, a_{t+1}) - Q_t(S_{1:t}, A_{1:t}) \right)^2 \right] + \lambda \Omega(Q_t) \quad (8)$$

for $t = T, T-1, \dots, 1$, where $\mathbb{E}_{|D|}$ is the empirical expectation, \mathcal{H}_t is a parameterized hypothesis space, $\Omega(Q_t)$ denotes some structures of Q_t , and λ is a tunable parameter to balance the empirical risk and structure. We then find a suitable \mathcal{H}_t and $\Omega(Q_t)$ so that \hat{Q}_t is close to Q_t^* .

In this section, we explain the proposed kernel-based distributed Q-learning for DTRs. Before presenting the detailed algorithm, we elucidate the reasons we use kernel-based Q-learning. This approach offers three main advantages:

- Q-learning can be regarded as a T -stage least squares regression problem, and kernel methods are well-developed learning schemes that exhibit optimal generalization performance (Caponnetto and De Vito 2007, Lin et al. 2017) in least squares regression, which implies that kernel methods perform excellently with strong theoretical guarantees in each stage.

- Numerous scalable variants of kernel methods have been proposed and successfully used, such as DKRR (Zhang et al. 2015), kernel learning with subsampling (Rudi et al. 2015), and localized SVM (Meister and Steinwart 2016). These variants provide guidance for the development of scalable Q-learning algorithms for DTRs.

- Linear spaces spanned by certain basis functions and deep neural networks are common hypothesis spaces in Q-learning (Sutton and Barto 2018). Due to their simple structures, linear

hypothesis spaces are beneficial for computations but have poor generalization performance. In addition, the complex structures of deep neural networks enable deep Q-learning in generalization but are frequently time consuming. Kernel methods balance Q-learning with linear spaces and deep Q-learning; kernelized Q-learning outperforms linear Q-learning in generalization and has a smaller computational burden than deep Q-learning.

Based on these, we use the well-known KRR (Caponnetto and De Vito 2007, Zhang et al. 2015) to derive an approximation of Q_t^* empirically based on the given dataset D . Let $K(x, x') := K_t(x, x')$ be a Mercer kernel, where $x, x' \in \mathcal{X}_t$, and $\mathcal{H}_{K,t}$ be the corresponding RKHS endowed with the norm $\|\cdot\|_{K,t}$. Given regularization parameters $\lambda_t, t = 1, \dots, T$, if we set $Q_{D, \lambda_{T+1}, T+1} = 0$ with $\lambda_{T+1} = 0$, then the Q -functions can be empirically defined by

$$Q_{D, \lambda_t, t} = \arg \min_{Q_t \in \mathcal{H}_{K,t}} \frac{1}{|D|} \sum_{i=1}^{|D|} (y_{i,t} - Q_t(x_{i,t}))^2 + \lambda_t \|Q_t\|_{K,t}^2, \quad t = T, T-1, \dots, 1, \quad (9)$$

where

$$y_{i,t} := r_{i,t} + \max_{a_{t+1} \in \mathcal{A}_{t+1}} Q_{D, \lambda_{t+1}, t+1}(s_{i,1:t+1}, a_{i,1:t}, a_{t+1}). \quad (10)$$

In this way, (9) can be solved backward to derive a sequence of estimators $\{Q_{D, \lambda_t, t}\}_{t=1}^T$. We then define the corresponding KRR for DTRs (KRR-DTR) by $\pi_{D, \vec{\lambda}} = (\pi_{D, \lambda_{1,1}}, \dots, \pi_{D, \lambda_{T,T}})$, where

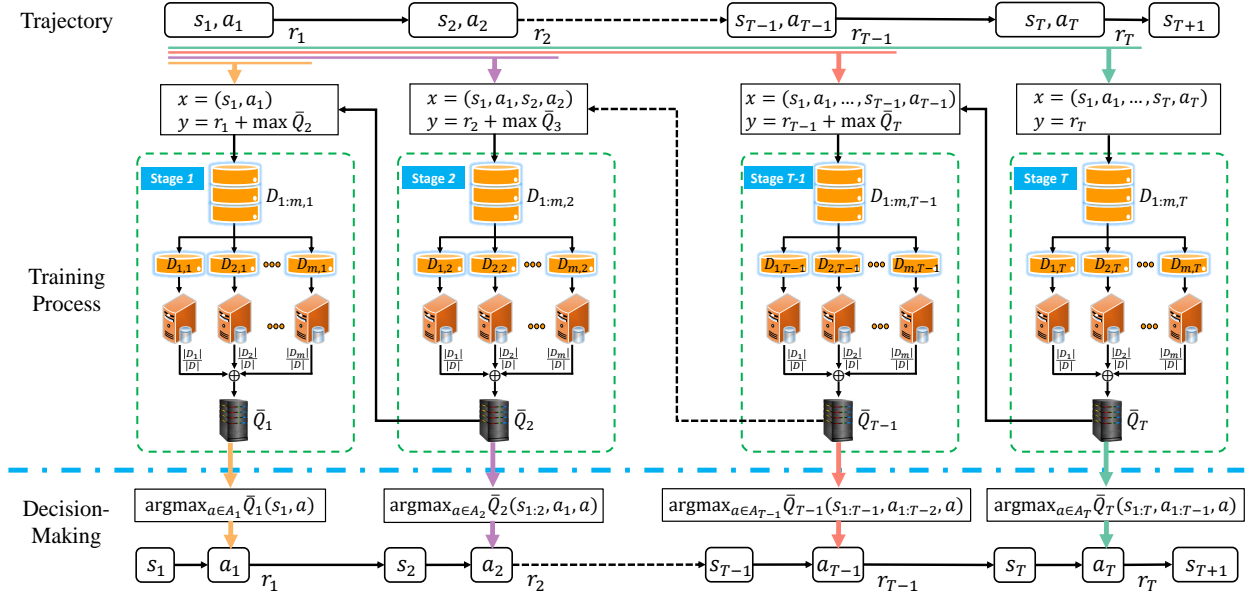
$$\pi_{D, \lambda_t, t}(s_{1:t}, a_{1:t-1}) = \arg \max_{a_t \in \mathcal{A}_t} Q_{D, \lambda_t, t}(s_{1:t}, a_{1:t-1}, a_t), \quad t = 1, \dots, T. \quad (11)$$

Solving KRR (9) requires $\mathcal{O}(|D|^3)$ floating computations in each stage, which makes KRR time consuming for large-scale datasets. A scalable variant of (9) should be developed to reduce the computational burden so that (9) can be successfully utilized to handle large-scale datasets to generate a high-quality DTR. Distributed learning equipped with a divide-and-conquer strategy (Zhang et al. 2015, Lin et al. 2017, 2020) is preferable for this purpose.

Kernel-based distributed Q-learning can be divided into four steps: division, local processing, synthesis, and iteration.

- *Division*: Randomly divide the dataset D into m disjoint subsets D_j according to the uniform distribution, that is, $D = \cup_{j=1}^m D_j$, $D_j \cap D_{j'} = \emptyset$ for $j \neq j'$. Denote $D_j = \{s_{i,j,1:T+1}, a_{i,j,1:T}, r_{i,j,1:T}\}_{i=1}^{|D_j|}$.

Figure 2 Training and decision-making flows of DKRR-DTR.



- *Local Processing*: Initialize $\bar{Q}_{D, \lambda_{T+1}, T+1} \equiv 0$, where $\lambda_{T+1} = 0$. At the t th stage, calculate the output of the i th sample in the j th data subset as

$$\bar{y}_{i,j,t} := r_{i,j,t} + \max_{a_{t+1} \in \mathcal{A}_{t+1}} \bar{Q}_{D, \lambda_{t+1}, t+1}(s_{i,j,1:t+1}, a_{i,j,1:t}, a_{t+1}), \quad j = 1, \dots, m, \quad (12)$$

and run KRR with parameter λ_t on the data D_j to obtain a local estimator of the Q-function

$$Q_{D_j, \lambda_t, t} = \arg \min_{Q_t \in \mathcal{H}_{K,t}} \frac{1}{|D_j|} \sum_{i=1}^{|D_j|} (\bar{y}_{i,j,t} - Q_t(s_{i,j,1:t}, a_{i,j,1:t}))^2 + \lambda_t \|Q_t\|_{K,t}^2, \quad j = 1, \dots, m. \quad (13)$$

- *Synthesis*: Synthesize the global estimator as

$$\bar{Q}_{D, \lambda_t, t} = \sum_{j=1}^m \frac{|D_j|}{|D|} Q_{D_j, \lambda_t, t}. \quad (14)$$

- *Iteration and Decision-Making*: Repeat the local processing and synthesis steps for $t = T, T-1, \dots, 1$, and obtain a set of Q-functions $\{\bar{Q}_{D, \lambda_t, t}\}_{t=1}^T$ based on DKRR. Define the DKRR for DTRs (DKRR-DTR) estimator by $\bar{\pi}_{D, \bar{\lambda}} = (\bar{\pi}_{D, \lambda_1, 1}, \dots, \bar{\pi}_{D, \lambda_T, T})$, where

$$\bar{\pi}_{D, \lambda_t, t}(s_{1:t}, a_{1:t-1}) = \arg \max_{a_t \in \mathcal{A}_t} \bar{Q}_{D, \lambda_t, t}(s_{1:t}, a_{1:t-1}, a_t), \quad t = 1, \dots, T. \quad (15)$$

The training and decision-making flows of the above approach are shown in Figure 2, where $D_{j,t}$ represents the data on the j th local machine at the t th stage and $\bar{Q}_{D, \lambda_t, t}$ is rewritten as \bar{Q}_t for

convenience. The detailed implementation of DKRR-DTR can also be found in Appendix B. A comparison of (14) with (9) shows that the computational complexity of KRR-DTR is reduced from $\mathcal{O}(|D|^3)$ to $(|D_j|^3)$ at each stage on the j th local machine. If the data subset sizes are the same, that is, $|D_1| = |D_2| = \dots = |D_m|$, then each local machine has only $\mathcal{O}(|D|^3/m^3)$ floating computations at each stage. If local processing is performed in parallel on a single machine, then $\mathcal{O}(|D|^3/m^2)$ floating computations are required. As in the classical regression setting (Zhang et al. 2015, Lin et al. 2017, Lin and Zhou 2018), the number of local machines m balances the generalization error and computational complexity of DKRR-DTR. A small m yields perfect generalization but needs huge computations, whereas a large m significantly accelerates the algorithm but may degrade its generalization performance. Therefore, it is crucial to theoretically derive some values of m with which DKRR-DTR performs similarly to KRR-DTR while reducing its computational burden.

4. Theoretical Behaviors

In this section, we deduce the generalization error of DKRR-DTR to quantify the relationship between the quality of DKRR-DTR and the number of samples. As a byproduct, the generalization error of KRR-DTR is derived as reference.

4.1. Assumptions

According to the “no free lunch” theory in statistical learning theory (Györfi et al. 2006, Theorem 3.1), satisfactory generalization error bounds cannot be derived for learning algorithms without any assumptions about the data. Therefore, some restrictions on the data D and the distribution P should be set for our analysis. Our first assumption focuses on the massiveness of the state and action spaces.

ASSUMPTION 1. *For any $t = 1, \dots, T$, \mathcal{S}_t is a compact set and \mathcal{A}_t is a finite set.*

The above assumption corresponds to Q-learning’s infinite states and finite treatment options in DTRs. Given Assumption 1, $\mathcal{X}_t = \mathcal{S}_{1:t} \times \mathcal{A}_{1:t}$ is also compact. Assumption 2 is established to quantify the relationship between the Q-functions and value functions in the setting of DTRs.

ASSUMPTION 2. Let $\mu \geq 1$ be a constant. It holds that

$$p_t(a|s_{1:t}, a_{1:t-1}) \geq \mu^{-1}, \quad \forall a \in \mathcal{A}_t, t = 1, \dots, T. \quad (16)$$

Assumption 2, a widely used assumption in the RL and dynamic treatment communities (Murphy 2005b, Qian and Murphy 2011, Goldberg and Kosorok 2012), declares that conditioned on previous treatment information, any action in the finite set \mathcal{A}_t can be chosen with a probability of at least μ^{-1} . Based on Assumption 2, it follows from (Goldberg and Kosorok 2012, Eq. (16)) that for an arbitrary $Q_t \in \mathcal{L}_t^2$, there holds

$$E[V_1^*(S_1) - V_{\pi,1}(S_1)] \leq \sum_{t=1}^T 2\mu^{t/2} \sqrt{E[(Q_t - Q_t^*)^2]} = \sum_{t=1}^T 2\mu^{t/2} \|Q_t - Q_t^*\|_{\mathcal{L}_t^2}, \quad (17)$$

where $\pi = (\pi_1, \dots, \pi_T)$ is defined by $\pi_t(s_{1:t}, a_{1:t-1}) = \arg \max_{a_t \in \mathcal{A}_t} Q_t(s_{1:t}, a_{1:t-1}, a_t)$. The relation (17) asserts that Q_t approaching Q_t^* implies $V_{\pi,1}$ approximating V_1^* well, provided that π is defined to maximize Q-functions. In this way, we can derive

$$E[V_1^*(S_1) - V_{\pi_{D,\bar{\lambda}},1}(S_1)|D] \leq 2 \sum_{t=1}^T \mu^{t/2} \|Q_{D,\lambda_t,t} - Q_t^*\|_{\mathcal{L}_t^2} \quad (18)$$

and

$$E[V_1^*(S_1) - V_{\bar{\pi}_{D,\bar{\lambda}},1}(S_1)|D] \leq 2 \sum_{t=1}^T \mu^{t/2} \|\bar{Q}_{D,\lambda_t,t} - Q_t^*\|_{\mathcal{L}_t^2}, \quad (19)$$

showing that the generalization errors of KRR-DTR and DKRR-DTR can be bounded by the differences between the derived Q-functions and optimal Q-functions, where $E[\cdot|D]$ denotes the expectation conditioned on D .

Our third assumption concerns the boundedness of the reward function R_t .

ASSUMPTION 3. There exists an $M \geq 1$ such that $\|R_t\|_{L^\infty} \leq M$ for any $t = 1, \dots, T$.

Assumption 3 is quite mild because R_t is manually presented and almost all widely used reward functions (Sutton and Barto 2018, Sugiyama 2015) satisfy this assumption. According to (4) and $Q_{T+1}^* = 0$, Assumption 3 implies that

$$|y_t^*| \leq (T - t + 1)M, \quad \|Q_t^*\|_{L^\infty} \leq (T - t + 1)M \quad (20)$$

holds almost surely for any $1 \leq t \leq T$, showing that the optimal Q -functions are also bounded.

Furthermore, some regularity property of Q_t^* is given to quantify the relationship between Q_t^* and the kernel K . For this purpose, we first define an integral operator from $\mathcal{H}_{K,t}$ to $\mathcal{H}_{K,t}$ (also from \mathcal{L}_t^2 to \mathcal{L}_t^2 if no confusion is made) as

$$L_{K,t}f(x) = \int_{\mathcal{X}_t} f(x')K(x, x')dP_t(x'). \quad (21)$$

For any positive-definite kernel $K(\cdot, \cdot)$, $L_{K,t}$ is easily verified to be a positive compact operator (Smale and Zhou 2004, 2005). Define $L_{K,t}^r$ as the r -th power of $L_{K,t}$ via spectral calculus (Smale and Zhou 2005). Assumption 4, which is standard in supervised learning (Caponnetto and De Vito 2007, Rudi et al. 2015, Zhang et al. 2015, Blanchard and Krämer 2016, Lin et al. 2017, Lin and Zhou 2018), describes the regularity of Q_t^* with respect to the kernel K .

ASSUMPTION 4. *For any $t = 1, \dots, T$, assume that*

$$Q_t^* := L_{K,t}^r h_t, \quad \text{for some } h_t \in \mathcal{L}_t^2, \quad r > 0, \quad (22)$$

where $L_{K,t}$ is the integral operator from \mathcal{L}_t^2 to \mathcal{L}_t^2 , as defined by (21).

The index r in (22) quantifies the regularity of Q_t^* . If $r = 0$, then (22) means $Q_t^* \in \mathcal{L}_t^2$, implying that there is no regularity of Q_t^* . If $r = 1/2$, then (22) is equivalent to $Q_t^* \in \mathcal{H}_{K,t}$ (Smale and Zhou 2005), showing that Q_t^* is in the RKHS associated with the kernel K . If $r > 1/2$, then (22) implies that Q_t^* is in other RKHSs in $\mathcal{H}_{K,t}$ corresponding to smoother kernels than K . Generally speaking, the larger the r value, the better the assumed regularity of Q_t^* . As indicated by (4), the regularity assumption of Q_t^* depends on the regularity of the reward function R_t . Furthermore, since the R_t in a DTR can be manually set before the learning process, the regularity of Q_t^* in Assumption 4 indeed includes a wide range of selection of R_t , including both the smooth and constant reward functions, and is much looser than the assumptions in existing literature (Murphy 2005b, Goldberg and Kosorok 2012, Oh et al. 2022), where Q_t^* is assumed to belong to linear spaces.

Finally, we impose a restriction on the kernel. For any t , define the effective dimension (Caponnetto and De Vito 2007) as

$$\mathcal{N}_t(\lambda) := \text{Tr}((\lambda I + L_{K,t})^{-1} L_{K,t}), \quad \lambda > 0,$$

where $\text{Tr}(L)$ is the trace of the operator L . The following assumption describes the property of K via the effective dimension.

ASSUMPTION 5. *There exists an $s \in (0, 1]$ such that*

$$\mathcal{N}_t(\lambda) \leq C_0 \lambda^{-s}, \quad \forall t = 1, 2, \dots, T, \quad (23)$$

where $C_0 \geq 1$ is a constant independent of λ .

From the definition of $\mathcal{N}_t(\lambda_t)$, (23) always holds for $C_0 = \kappa := \max_{t=1, \dots, T} \sqrt{\sup_{x \in \mathcal{X}_t} K(x, x)}$ and $s = 1$. Therefore, without this assumption, our results below always hold for $s = 1$. This assumption is introduced to encode the property of the kernel in our theoretical analysis to make the established generalization error bounds more delicate. In particular, Assumption 5 is equivalent to the eigenvalue decay assumption in previous studies (Caponnetto and De Vito 2007, Zhang et al. 2015) and has been widely adopted in studies on kernel learning (Blanchard and Krämer 2016, Lin et al. 2017, Guo et al. 2017, Lu et al. 2020, Shi 2019).

In summary, five assumptions are involved in our analysis: Assumptions 1 and 2 are concerning the data D , Assumptions 3 and 4 are concerning the optimal Q-function Q_t^* , and Assumption 5 is concerning the kernel K . These assumptions can be simultaneously satisfied easily. For example, assume the state space is $\mathcal{S}_t := [0, 1]$ and the action space is $\{0, 1\}$; conditioned on $s_{1:t}, a_{1:t-1}$, one adopts the decision $a_t = 1$ with probability $1/2$ and the reward function $R_t(x) \equiv C$ for some constant C . If we adopt the Sobolev kernel $K(x_t, x'_t) = \max\{x_t \cdot x'_t, 1 - x_t \cdot x'_t\}$, then the above assumptions hold simultaneously with $\mu = 2$, $M = C$, $r = 1$, and $s = 1$.

4.2. Generalization error analysis

Before presenting the theoretical guarantees of DKRR-DTR, we first bound the generalization error of KRR-DTR to show the power of kernel-based Q-learning. The following theorem is our first theoretical result.

THEOREM 1. *Under Assumptions 1-5, with $\frac{1}{2} \leq r \leq 1$ and $0 < s \leq 1$, if $\lambda_1 = \dots = \lambda_T = |D|^{-\frac{1}{2r+s}}$, then*

$$E \left[V_1^*(S_1) - V_{\pi_{D,\bar{\lambda},1}}(S_1) \right] \leq C_1(T, \mu) |D|^{-\frac{r}{2r+s}}, \quad (24)$$

where

$$C_1(T, \mu) := C_1(2\mu\bar{C})^T T \sum_{t=1}^T 2^{-t} \sum_{\ell=t}^T \prod_{k=\ell}^{T-1} ((T-k+2)(2\mu^{1/2})^{k-\ell} + 1),$$

and \bar{C} and C_1 are constants depending only on M , C_0 , κ , r , s , and $\max_{t=1, \dots, T} \|h_t\|_{\mathcal{L}_t^2}$.

Theorem 1 quantifies the generalization error of KRR-DTR and the data size. According to (24), the generalization error of KRR-DTR decreases with respect to the data size. Moreover, it depends heavily on the regularity of the optimal Q-functions and the property of the adopted kernel. In particular, the better the regularity of Q_t^* , the smaller the generalization error; the smaller the effective dimension of the kernel, the better the quality of KRR-DTR. The derived rate $\mathcal{O}(|D|^{-\frac{r}{2r+s}})$ is the same as that for the classical KRR for regression in supervised learning (Caponnetto and De Vito 2007, Lin et al. 2017) under similar assumptions. The derived generalization error is dimensionality independent, showing that using kernel methods in Q-learning is essentially better than linear approaches.

From Theorem 1, the constant $C_1(T, \mu)$ behaves exponentially with respect to the horizon T , which is different from the results in (Fan et al. 2020). The main reason is that, except for the mild restriction in Assumption 2, we do not impose any restrictions on the distribution P , unlike (Fan et al. 2020). This property makes our analysis suitable only for Q-learning with a small T , coinciding with the practical implementation requirements of DTR in Table 1. Additional restrictions on P , such as the concentration-type assumption in (Fan et al. 2020) and margin-type assumption in (Oh et al. 2022), can improve the constant $C_1(T, \mu)$ and the convergence rate $|D|^{-\frac{r}{2r+s}}$. However, as these assumptions are difficult to satisfy in practice for DTRs, we do not use them in the present paper.

The derived generalization error bounds in (24) are much better than those for linear Q-learning (Murphy 2005b, Oh et al. 2022) in three aspects. First, we only impose the regularity assumption

(22) on optimal Q-functions, whereas Murphy (2005b) and Oh et al. (2022) required Q_t^* to belong to a linear combination of finite basis functions. The space of Q_t^* satisfying Assumption 4 is much more massive than the linear space studied in (Murphy 2005b) and (Oh et al. 2022). Second, the derived convergence rate $|D|^{-r/(2r+s)}$ is better than those established for linear Q-learning in previous studies, where rates slower than $|D|^{-1/4}$ were derived under stricter assumptions. For sufficiently small values of s , our derived rates can be of the order $|D|^{-1/2}$. Finally, due to linearity, the rates established in (Murphy 2005b) and (Oh et al. 2022) depend heavily on the dimension d , whereas our results are dimensionality independent, showing the power of kernelization.

Our next theoretical result presents a solid theoretical guarantee for the feasibility of DKRR-DTR.

THEOREM 2. *Under Assumptions 1-5, with $\frac{1}{2} \leq r \leq 1$ and $0 < s \leq 1$, if $\lambda_1 = \dots = \lambda_T = |D|^{-\frac{1}{2r+s}}$, $|D_1| = \dots = |D_m|$, and*

$$m(\log m + 1) \leq \frac{|D|^{\frac{2r+s-1}{4r+2s}}}{\log |D|}, \quad (25)$$

then

$$E \left[V_1^*(S_1) - V_{\bar{\pi}_{D,\bar{\lambda},1}}(S_1) \right] \leq C_2(T, \mu) |D|^{-\frac{r}{2r+s}}, \quad (26)$$

where

$$C_2(T, \mu) := C_2(2\mu\hat{C})^T T \sum_{t=1}^T 2^{-t} \sum_{\ell=t}^T \prod_{k=\ell}^{T-1} ((T-k+2)(2\mu^{1/2})^{k-\ell} + 1),$$

and \hat{C} and C_2 are constants depending only on M , C_0 , κ , r , s , and $\max_{t=1,\dots,T} \|h_t\|_{\mathcal{L}_t^2}$.

Theorem 2 presents a sufficient condition of m to guarantee the excellent generalization performance of DKRR-DTR. In particular, if the number of data subsets m and the total number of samples $|D|$ satisfy the relation (25), then DKRR-DTR performs almost the same as KRR-DTR, showing that the computation reduction approach made by distributed learning does not degrade the generalization performance of KRR-DTR. The restriction on m , such as (25), is necessary because the generalization performance of KRR-DTR cannot be realized if we use DKRR-DTR with each data subset containing only a few samples. An extreme case is $m = |D|$ where each data subset contains only one sample and DKRR-DTR cannot perform well.

Theorem 2 shows that DKRR-DTR possesses all the advantages of KRR-DTR, but its training cost is only $\mathcal{O}(|D|^3/m^3) \times m = \mathcal{O}(|D|^3/m^2)$, which is $1/m^2$ times smaller than that of KRR-DTR. Given that the quality of Q-learning algorithms is measured by their generalization performance, computation costs, and stability, the above assertions show that DKRR-DTR is better than linear Q-learning in generalization, better than deep Q-learning and KRR-DTR in computation, and better than deep Q-learning in stability as the optimization model defined by (13) can be analytically solved, whereas obtaining global minima with high-quality deep neural networks remains an open question in the realm of deep learning (Goodfellow et al. 2016, Chap.8). These findings illustrate that DKRR-DTR is a promising approach to yielding high-quality DTRs.

5. Simulations

In this section, two types of clinical trials for cancer treatment are simulated to demonstrate the efficacy of the proposed method compared with linear least squares-based and deep neural network-based Q-learning for DTRs (LS-DTR and DNN-DTR, respectively). The first simulation aims to find treatment regimes to maximize the survival time in the clinical trial with a flexible number of stages and a small number of actions; the second simulation aims to develop a policy of the injection dose levels of a single drug to maximize the cumulative survival probability (CSP) in the clinical trial with a large number of actions that are discretized from a continuous action space. For a fair comparison, we explain the implementation details and the parameters that should be tuned.

- In the training process of distributed Q-learning, training samples are randomly and equally distributed to local machines; the time of data transmission from different local machines is not considered; the computing capabilities of the local machines are assumed to be the same for simplicity.
- For DNN-DTR, a fully connected feed-forward network with a sigmoid activation function and Xavier initialization (Glorot and Bengio 2010) is employed to estimate Q-functions; the number of hidden layers, the number of neurons in the hidden layers, and the number of epochs of DNN are tuned parameters, and the other important settings are listed in Table 2.

Table 2 Default values of parameters in DNN.

Optimizer	Momentum	Learning rate	Batch size	Weight decay	Loss
SGDM	0.9	0.05	5000	0.0001	MSELoss

- For KRR-DTR and DKRR-DTR, the positive-definite function $\phi(x_1, x_2) = \exp(-\frac{\|x_1 - x_2\|_2^2}{2\sigma^2})$ is used as the kernel function; the kernel width σ and the coefficient λ of ℓ^2 regularization are tuned parameters.

- The value of the same parameter is maintained at all clinical stages; the parameters that require tuning are chosen by grid search to maximize the specific target (such as the expected survival time or CSP).

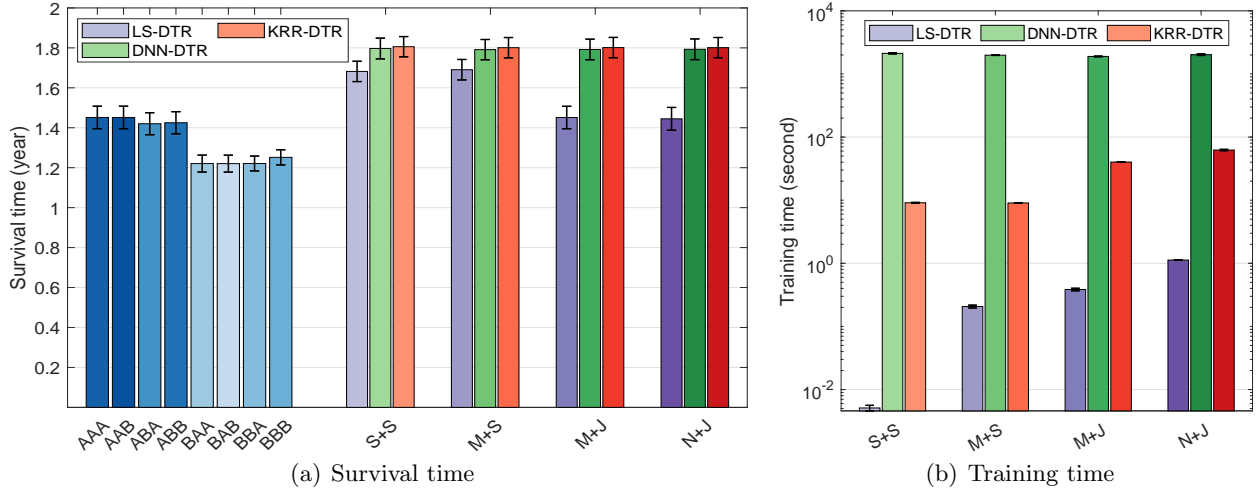
All simulations are run on a desktop workstation equipped with an Intel(R) Core(TM) i9-10980XE 3.00 GHz CPU, an Nvidia GeForce RTX 3090 GPU, 128 GB of RAM, and Windows 10; the DNN-DTR programs are executed on the GPU, and the others are executed on the CPU. The results are recorded by averaging the results from multiple individual trials with the best parameters.

5.1. Clinical trial with a small number of treatment options

Patients with NSCLC typically undergo one to three treatment lines. The number of treatments is flexible because the disease progression and the therapy tolerance ability of patients are different. In this simulation, we consider the problem of developing an optimal treatment policy that maximizes the expected survival time.

We use the mathematical model of cancer dynamics proposed by Goldberg and Kosorok (2012) to generate the clinical trajectory, where the treatment options include an aggressive treatment A and a conservative treatment B . The details of trajectory generation are described in Appendix C. The following cases are considered to examine the performance of the proposed method:

- The state s_i is the wellness w_i at the start of the i th stage, and the Q-functions at the i th stage are estimated separately as functions of the state s_i for actions A and B ; we refer to this case as “single feature + separately” (S+S).

Figure 3 Survival and training times of methods with batch-mode training of all data.

- The state s_i is composed of the wellness w_i at the start of the i th stage and the reward r_{i-1} of the $(i-1)$ th stage, that is, $s_i = (w_i, r_{i-1})$, where $r_0 \equiv 0$, and the Q-functions at the i th stage are estimated separately as functions of the state s_i for actions A and B ; we refer to this case as “multiple feature + separately” (M+S).

- The state s_i is composed of the wellness w_i and reward r_{i-1} , that is, $s_i = (w_i, r_{i-1})$, and the Q-function at the i th stage is estimated as a joint function of the state s_i and the action a_i ; we refer to this case as “multiple feature + jointly” (M+J).

- The state s_i is composed of the wellness w_i and reward r_{i-1} , that is, $s_i = (w_i, r_{i-1})$, and the Q-function at the i th stage is estimated as a joint function of the states and actions of all stages up to stage i ; we refer to this case as “non-Markovian + jointly” (N+J).

The experimental settings of the simulation are first introduced. We generate a dataset of $N = 10000$ trajectories for training and tested the policy $\pi = (\pi_1, \pi_2, \pi_3)$ by generating 1000 new trajectories in which the treatment of the i th stage accords with π_i . For KRR-DRT and DKRR-DRT, the parameter λ is chosen from the set $\{\frac{1}{2^q} | \frac{1}{2^q} > \frac{1}{2^N}, q = 0, 1, 2, \dots\}$, and the kernel width σ is chosen from a set of 20 values drawn in an equally spaced logarithmic interval $[0.001, 1]$. For DNN-DRT, the number of hidden layers, the neuron number in the hidden layers, and the number of epochs are chosen from the sets $\{1, 2, 3, 4\}$, $\{10, 20, \dots, 100\}$, and $\{2000, 4000, \dots, 10000\}$, respectively. LS-DRT

has no parameters that require tuning. The expected value of survival time is estimated using the mean of the survival time of the 1000 patients. For each method with the best parameters, we conduct the simulation 500 times and record the average value of the estimated mean survival time for evaluation.¹ In the following, we give some comparisons from aspects of nondistributed and distributed Q-learning.

- *Nondistributed Q-learning*: We compare LS-DTR, DNN-DTR, and KRR-DTR with eight fixed treatments ($a_1a_2a_3$ for $a_i \in \{A, B\}$). The comparisons of survival and training times are shown in Figure 3, from which we can conclude the following: 1) The policies AAA and AAB have the best survival time among the eight fixed treatments, but they are still significantly worse than the policies obtained by the Q-learning methods, which illustrates the power of RL in discovering effective regimens for life-threatening diseases. 2) LS-DTR has the shortest training time, which increases from case S+S to case N+J. This is because the training complexity of LS-DTR is independent of the number of training samples; it is only related to the dimension of the data input (the dimension increases from case S+S to case N+J). Nevertheless, LS-DTR has the worst survival time among the three Q-learning methods. The survival times of LS-DTR for cases S+S and M+S are obviously higher than those of LS-DTR for cases M+J and N+J, which indicates that LS is not good at jointly handling states and actions when the size of the action space is small. 3) KRR-DTR performs similarly to (or slightly better than) DNN-DTR in terms of survival time, although it takes between one hundredth and tenth as long to train as DNN-DTR. 4) From case S+S to case N+J, the training time of KRR-DTR increases because the complexity of kernel computation is related to the dimension of the data input; the training time of DNN-DTR is almost unchanged because it mainly focuses on the numbers of training samples and epochs, and calculations related to data dimension can be ignored. Although KRR-DTR has the best performance in terms of both survival time and training cost in this simulation, it is unsuitable for large-scale data because of the high storage requirements of the kernel matrix and the high computational complexity of solving KRR problems. Thus, we develop a DKRR Q-learning approach.

¹ The DNN-DTR simulation is conducted 100 times because of the high training cost.

Table 3 Computational complexity of training flow in Appendix B. INDV represents the complexity of calculating each individual item; TOT represents the total complexity of Step 6, the loop from Step 8 to Step 10, the loop from Step 12 to Step 15, and Step 17. $M_{D_j,t,\lambda_j,t} = (\mathbb{K}_{D_j,t,D_j,t} + \lambda|D_j|\mathbb{I}_{D_j,t})^{-1}$, and $\vec{\alpha}_{j,t} = M_{D_j,t,\lambda_j,t}\vec{Y}_{D_j,\vec{\lambda}_{t+1},t}$.

Item	Step 6			Steps 8–10		Steps 12–15	Step 17
	$\mathbb{K}_{D_j,t,D_j,t}$	$M_{D_j,t,\lambda_j,t}$	$\vec{\alpha}_{j,t}$	$\mathbb{K}_{D_k,t,D_j,t}$	$\vec{H}_{D_j,k,a,t}$	$\vec{H}_{D,k,a,t}$	$\vec{Y}_{D_j,\vec{\lambda}_t,t-1}$
INDV	$\frac{N^2\kappa_t}{m^2}$	$\frac{N^3}{m^3}$	$\frac{N^2}{m^2}$	$\frac{N^2\kappa_t}{m^2}$	$\frac{N^2}{m^2}$	N	$\frac{N}{m}$
TOT	$O\left(\frac{N^2\kappa_t}{m^2} + \frac{N^3}{m^3} + \frac{N^2}{m^2}\right)$			$O\left(\frac{N^2\kappa_t\ell_t}{m} + \frac{N^2}{m}\ell_t\right)$		$O(\ell_t m N)$	$O\left(\frac{N}{m}\right)$

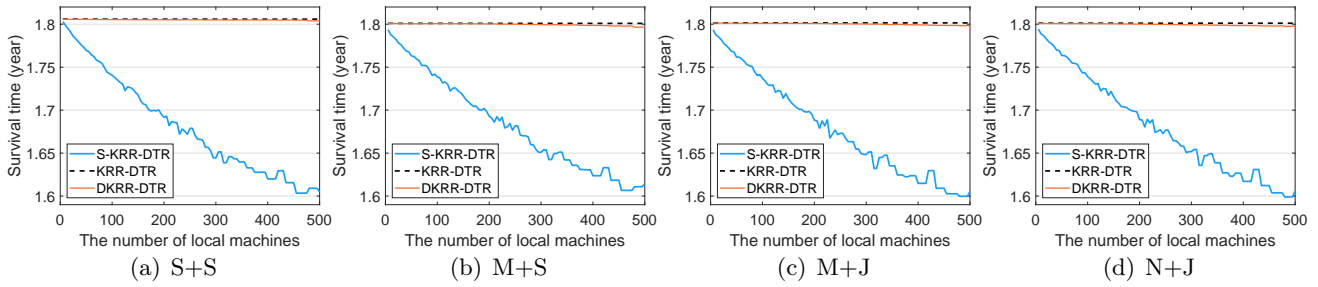
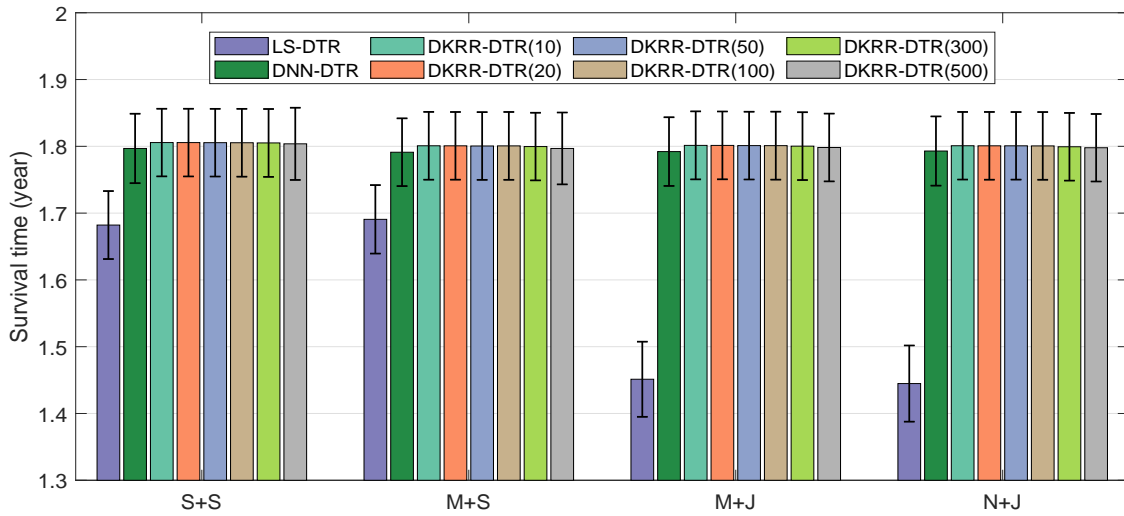
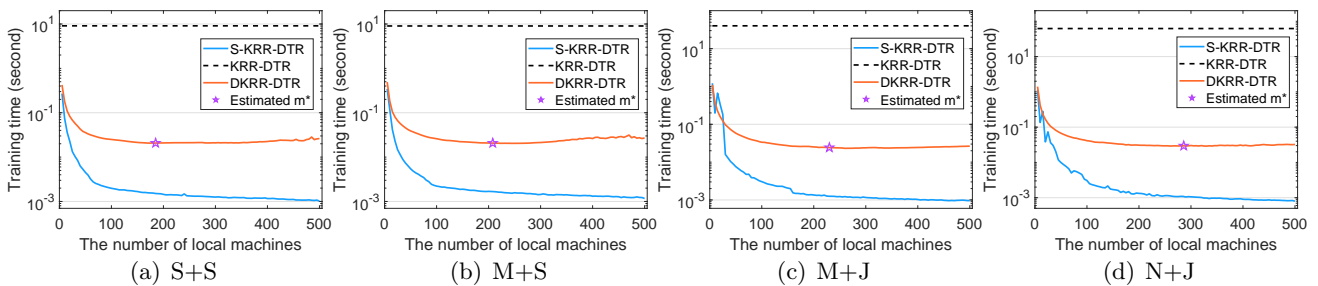
• *Distributed Q-learning*: The computational complexity of the training flow of DKRR-DTR in Appendix A is theoretically analyzed in Table 3, in which the computational complexities of Steps 6, 8–10, and 17 refer to those on each local machine, provided that parallelization is implemented. The time of data transmission in Steps 7, 9, and 14 is not considered. Thus, the training complexity of DKRR-DTR is $O\left(TN^3/m^3 + \left(\sum_{t=1}^T \ell_t(1 + \kappa_t)\right)N^2/m + \left(\sum_{t=1}^T \ell_t\right)Nm\right)$, where κ_t represents the complexity of calculating a kernel value at the t th stage and ℓ_t represents the number of actions in the action space \mathcal{A}_t . We define the function of training complexity as

$$\Omega_{\text{DKRR-DTR}}(m) = TN^3/m^3 + \left(\sum_{t=1}^T \ell_t(1 + \kappa_t)\right)N^2/m + \left(\sum_{t=1}^T \ell_t\right)Nm, \quad (27)$$

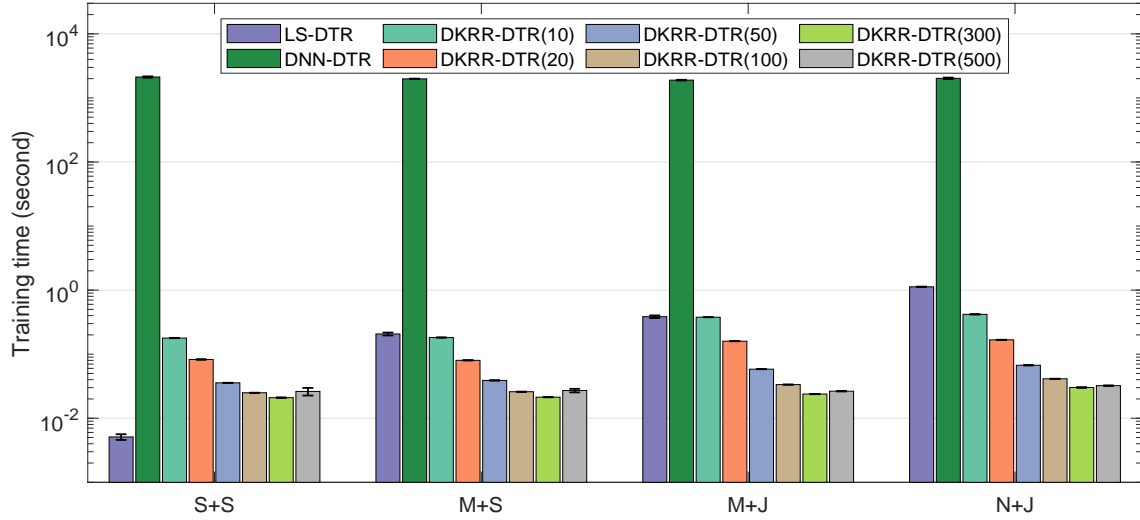
where the first two terms are related to the training complexity on each local machine, and the last term is related to the training complexity of synthesis on the global machine. The function $\Omega_{\text{DKRR-DTR}}(m)$ decreases and then increases as m increases because when the number m of local machines is large enough, the marginal utility of reducing the training time is very small, whereas training complexity focuses primarily on synthesis. Naturally, the number m with the smallest $\Omega_{\text{DKRR-DTR}}(m)$ can be written as

$$m^* = \sqrt{\frac{\sqrt{\left(\sum_{t=1}^T \ell_t(1 + \kappa_t)\right)^2 + 12T\left(\sum_{t=1}^T \ell_t\right) + \sum_{t=1}^T \ell_t(1 + \kappa_t)}}{2\left(\sum_{t=1}^T \ell_t\right)}}\sqrt{N}, \quad (28)$$

which is a good estimate of the optimal number of local machines in parallel computing. Once the data and kernel function are provided, the complexity κ_t of computing a kernel value can be considered a constant related to the dimension of the data input.

Figure 4 Relation between survival time and the number of local machines for DKRR-DTR.**Figure 5** Survival time of LS-DTR, DNN-DTR, and DKRR-DTR with different numbers of local machines.**Figure 6** Relation between training time and the number of local machines for DKRR-DTR.

To verify the above analysis of computational complexity and examine the efficacy of DKRR-DTR, we vary the number m of local machines from the set $\{5, 10, \dots, 500\}$ in the simulation. Experiments are conducted on KRR-DTR with a single machine (denoted by S-KRR-DTR), in which the number of training samples is equal to that of each local machine in DKRR-DTR, to provide a baseline for assessing the performance of DKRR-DTR. The relation between survival time and the number of

Figure 7 Training time of LS-DTR, DNN-DTR, and DKRR-DTR with different numbers of local machines.

local machines is shown in Figure 4, and the survival time of LS-DTR, DNN-DTR, and DKRR-DTR with different numbers of local machines is shown in Figure 5, in which the numbers in brackets after the notation DKRR-DTR are the numbers of local machines. The corresponding training time is shown in Figures 6 and 7. From the above results, we have the following observations: 1) As the number of local machines grows, the survival time of S-KRR-DTR decreases dramatically, since there are fewer training samples on a single machine. By contrast, the survival time of DKRR-DTR is almost unchanged; even with 500 local machines, the performance of DKRR-DTR remains superior to that of DNN-DTR and LS-DTR and is nearly identical to that of KRR-DTR, which trains all data in batch mode. 2) In all four cases, the curves of training time of DKRR-DTR drop sharply and then rise slowly as the number of local machines increases, which verifies the complexity deduced in (27). The points whose coordinates are composed of the estimated m^* by (28) and the corresponding training time of DKRR-DTR are marked by purple pentagrams in Figure 6. The training time with the estimated number m^* is very close to the minimum training time, which validates the correctness and reliability of (28). 3) The training complexity of DKRR-DTR is higher than that of S-KRR-DTR (especially for large values of m) because S-KRR-DTR does not have synthesis steps, but it is evidently lower than that of DNN-DTR, that is, the training time of DKRR-DTR is one thousandth (or even one ten thousandth) of that of DNN-DTR. When m is

larger than 10, the training time of DKRR-DTR (in all cases except S+S) is even less than that of LS-DTR, whose training complexity is independent of training data size. Overall, DKRR-DTR is highly efficient in the training stage while generalizing comparably to KRR-DTR and DNN-DTR, which implies that DKRR-DTR can be applied to large-scale Q-learning problems.

5.2. Clinical trial with a large number of treatment options

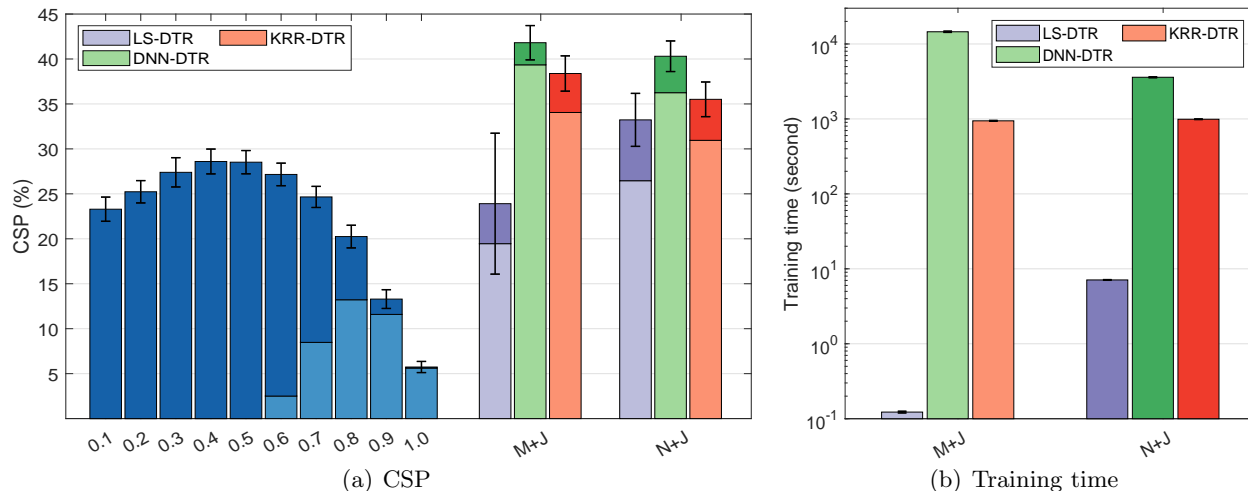
This simulation considers a clinical trial with a fixed length of treatment stages; each patient undergoes a treatment at a specific time point in each course (a month is a course, and a treatment is applied to the patient at the beginning of each month). The treatment set consists of a large number of dose levels that are discretized from the continuous dose-level intervals of a single drug. We design an optimal treatment strategy that considers a drug’s efficacy and toxicity simultaneously to maximize the CSP after all treatment courses.

We use the model proposed by Zhao et al. (2009) to simulate cancer dynamics and generate clinical trajectory data. The details of the simulated data are given in Appendix D. The action space consists of a large number of dose levels; therefore, we only consider the following cases:

- The state s_i consists of the toxicity w_i and tumor size m_i at the i th stage, that is, $s_i = (w_i, m_i)$, and the Q-function at the i th stage is estimated as a joint function of the state s_i and action a_i ; we refer to this case as “Markovian + jointly” (M+J).

- The state s_i consists of the toxicity w_i and tumor size m_i at the i th stage, that is, $s_i = (w_i, m_i)$, and the Q-function at the i th stage is estimated as a joint function of the states and actions of all stages up to stage i ; we refer to this case as “non-Markovian + jointly” (N+J).

The settings of this simulation are as follows. We generate $N = 20000$ trajectories for training and 1000 trajectories for evaluation. For KRR-DRT and DKRR-DRT, the parameter λ is chosen from the set $\{\frac{1}{2^q} | \frac{100}{N} > \frac{1}{2^q} > \frac{1}{10N}, q = 0, 1, 2, \dots\}$, and the kernel width σ is chosen from a set of 20 values drawn in an equally spaced logarithmic interval $[0.01, 10]$. For DNN-DRT, the parameter ranges are the same as those in Section 5.1. The expected CSP value is estimated using the mean CSP value of the 1000 patients. The simulation is conducted 100 times for each method with the best

Figure 8 CSP and training time of methods with batch-mode training of all data.

parameters, and the average value of the estimated mean CSP is reported for comparison.² We also give some comparisons from aspects of nondistributed and distributed Q-learning approaches.

- *Nondistributed Q-learning*: We compare LS-DTR, DNN-DTR, and KRR-DTR with 10 fixed treatments whose dose levels range from 0.1 to 1.0 in increments of 0.1. Comparisons of the CSP and training time are shown in Figure 8, where the light and dark shades of each color series represent the cumulative cured probability (CCP) and trial end probability (TEP) of the compared methods. Here, the CCP is the proportion of patients cured in the treatment cycle, and TEP is the proportion of patients alive but not cured at the end of the trial. From the results, we obtain the following observations: 1) Some fixed treatments, such as dose levels of 0.3 – 0.6, have good CSP values and even outperform LS-DTR in the case of M+J. However, their CCP values are evidently lower than those of Q-learning methods. The CCP is usually more important than TEP because patients prefer to be cured in the treatment cycle. Hence, RL can provide effective treatment policies for life-threatening diseases. 2) Among the three Q-learning methods, DNN-DTR performs the best because of its excellent nonlinear fitting capability, although it has the longest training time. LS-DTR has the shortest training time; the CSP value of LS-DTR in the case of N+J is significantly better than that in M+J due to the expansion of the linear hypothesis space (the dimension of data

² The DNN-DTR and DKRR-DTR simulations are conducted 20 times.

Figure 9 Relation between CSP (training time) and the number of local machines in DKRR-DTR.

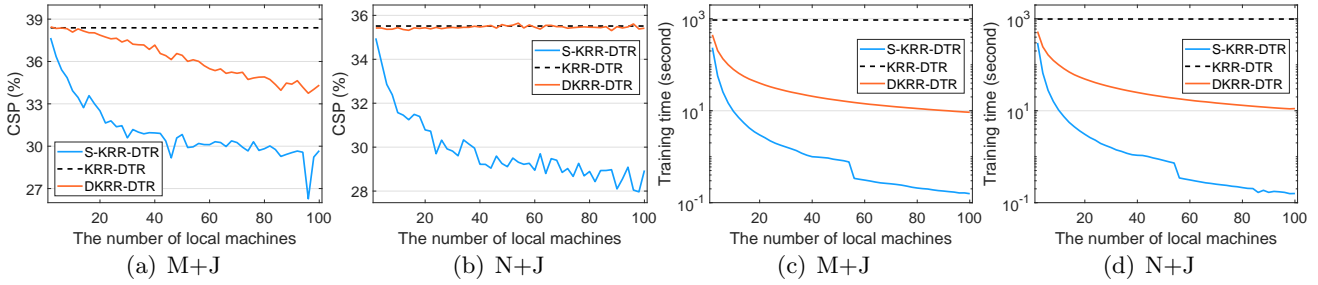
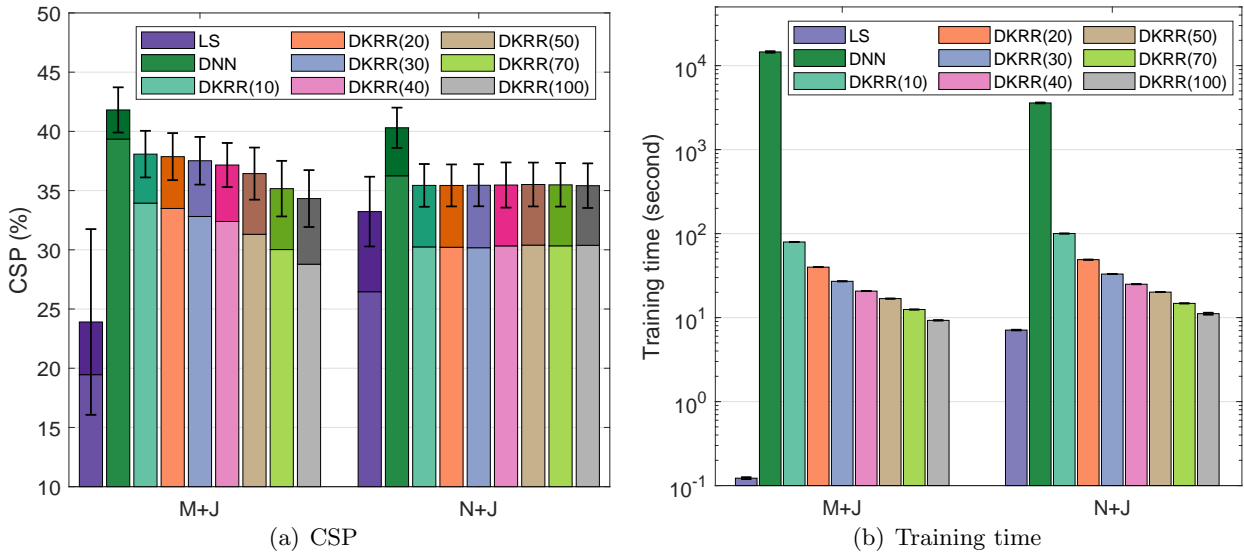


Figure 10 CSP and training time of LS-DTR, DNN-DTR, and DKRR-DTR with different numbers of local machines.



input grows with the number of stages in N+J), but LS-DTR still has the lowest CSP values and the highest standard deviations. KRR-DTR is a compromise between the CSP and training time; its CSP value is slightly smaller than that of DNN-DTR, but it is more efficient than DNN-DTR. The CSP values of DNN-DTR and KRR-DTR in N+J are slightly smaller than those in M+J. This may be because the Markovian assumption holds for this simulation, and training DNN and KRR using data with large dimensions is difficult. The advantage of KRR-DTR over DNN-DTR in terms of training time is not particularly significant because the training complexity of KRR-DTR is proportional to the cube of the number of training samples, making DKRR-DTR imperative.

- *Distributed Q-learning*: The efficiency and effectiveness of DKRR-DTR are evaluated by varying the number m of local machines from the set $\{2, 4, \dots, 100\}$ in the simulation. The relationship

of the CSP and training time against the number of local machines is shown in Figure 9, and comparisons of the CSP and training time of LS-DTR, DNN-DTR, and DKRR-DTR with different numbers of local machines are shown in Figure 10, in which LS-DTR, DNN-DTR, and DKRR-DTR are abbreviated as LS, DNN, and DKRR, respectfully, for brevity. Based on the above results, we have the following assertions: 1) The CSP value of DKRR-DTR decreases slowly as the number m of local machines increases; even m reaches 40, it is still satisfactory compared with KRR-DTR with batch-mode training of all data. Moreover, the increasing m greatly reduces training complexity, which overcomes the drawback of KRR-DTR. 2) Although DNN-DTR has a better CSP than DKRR-DTR, its training time is several orders of magnitude larger than that of DKRR-DTR. DKRR-DTR gives a perfect balance between training complexity and generalization performance, which makes it feasible and effective to implement Q-learning with large amounts of data.

These simulations illustrate that DKRR-DTR has higher efficiency and superior performance in dealing with large-scale Q-learning problems compared with state-of-the-art methods, such as LS-DTR and DNN-DTR.

References

- Almirall D, Chronis-Tuscano A (2016) Adaptive interventions in child and adolescent mental health. *Journal of Clinical Child and Adolescent Psychology* 45(4):383–395.
- Bastani H, Bayati M (2020) Online decision making with high-dimensional covariates. *Operations Research* 68(1):276–294.
- Blanchard G, Krämer N (2016) Convergence rates of kernel conjugate gradient for random design regression. *Analysis and Applications* 14(06):763–794.
- Breiman L (2001) Random forests. *Machine Learning* 45:5–32.
- Breiman L, Friedman JH, Olshen R, Stone C (1984) *Classification and Regression Trees* (Monterey: CRC Press).
- Caponnetto A, De Vito E (2007) Optimal rates for the regularized least-squares algorithm. *Foundations of Computational Mathematics* 7(3):331–368.

-
- Chakraborty B, Moodie EEM (2013) *Statistical Reinforcement Learning* (New York: Springer).
- Chakraborty B, Murphy SA (2014) Dynamic treatment regimes. *Annual Review of Statistics and Its Application* 1:447–464.
- Chang X, Lin SB, Zhou DX (2017) Distributed semi-supervised learning with kernel ridge regression. *The Journal of Machine Learning Research* 18(1):1493–1514.
- Consortium IWP (2009) Estimation of the warfarin dose with clinical and pharmacogenetic data. *New England Journal of Medicine* 360(8):753–764.
- Cucker F, Zhou DX (2007) *Learning Theory: An Approximation Theory Viewpoint*, volume 24 (Cambridge University Press).
- Ernst D, Geurts P, Wehenkel L (2005) Tree-based batch mode reinforcement learning. *Journal of Machine Learning Research* 6:503–556.
- Even-Dar E, Mansour Y (2003) Learning rates for q-learning. *Journal of Machine Learning Research* 5(Dec):1–25.
- Evgeniou T, Pontil M, Poggio T (2000) Regularization networks and support vector machines. *Advances in Computational Mathematics* 13(1):1–50.
- Fan J, Yang Z, Xie Y, Wang Z (2020) A theoretical analysis of deep q-learning. *arXiv preprint arXiv:1901.00137v3* .
- François-Lavet V, Henderson P, Islam R, Bellemare MG, Pineau J, et al. (2018) An introduction to deep reinforcement learning. *Foundations and Trends in Machine Learning* 11(3-4):219–354.
- Friedman JH (1991) Multivariate adaptive regression splines. *The Annals of Statistics* 19(1):1–67.
- Gittens A, Mahoney MW (2016) Revisiting the nyström method for improved large-scale machine learning. *The Journal of Machine Learning Research* 17(1):3977–4041.
- Glorot X, Bengio Y (2010) Understanding the difficulty of training deep feedforward neural networks. *Proceedings of the 13th International Conference on Artificial Intelligence and Statistics*, 249—356 (Sardinia, Italy).
- Goldberg Y, Kosorok MR (2012) Q-learning with censored data. *The Annals of Statistics* 40(1):529–560.

- Goodfellow I, Bengio Y, Courville A (2016) *Deep Learning* (MIT Press).
- Gosavi A (2009) Reinforcement learning: A tutorial survey and recent advances. *INFORMS Journal on Computing* 21(2):178–192.
- Guo ZC, Lin SB, Zhou DX (2017) Learning theory of distributed spectral algorithms. *Inverse Problems* 33(7):074009.
- Györfi L, Kohler M, Krzyzak A, Walk H (2006) *A Distribution-Free Theory of Nonparametric Regression* (Springer Science & Business Media).
- Humphrey K (2017) *Using reinforcement learning to personalize dosing strategies in a simulated cancer trial with high dimensional data*. Master’s thesis, The University of Arizona, Tucson, URL <http://hdl.handle.net/10150/625341>.
- Ishigooka J, Murasaki M, Miura S, Group TOLPIS (2000) Olanzapine optimal dose: Results of an open-label multicenter study in schizophrenic patients. *Psychiatry and Clinical Neurosciences* 54(4):467–478.
- Kalashnikov D, Irpan A, Pastor P, Ibarz J, Herzog A, Jang E, Quillen D, Holly E, Kalakrishnan M, Vanhoucke V, et al. (2018) Qt-opt: Scalable deep reinforcement learning for vision-based robotic manipulation. *arXiv preprint arXiv:1806.10293* .
- Kearns MJ, Singh SP (1999) Finite-sample convergence rates for q-learning and indirect algorithms. *Advances in Neural Information Processing Systems*, 996–1002.
- Kraus M, Feuerriegel S, Oztekin A (2020) Deep learning in business analytics and operations research: Models, applications and managerial implications. *European Journal of Operational Research* 281(3):628–641.
- Lavori PW, Dawson R (2008) Adaptive treatment strategies in chronic disease. *Annual Review of Medicine* 59(1):443–453.
- Lin SB, Guo X, Zhou DX (2017) Distributed learning with regularized least squares. *The Journal of Machine Learning Research* 18(1):3202–3232.
- Lin SB, Wang D, Zhou DX (2020) Distributed kernel ridge regression with communications. *J. Mach. Learn. Res.* 21:93–1.
- Lin SB, Zhou DX (2018) Distributed kernel-based gradient descent algorithms. *Constructive Approximation* 47(2):249–276.

-
- Liu S, Su H (2022) Provably efficient kernelized q-learning. *arXiv preprint arXiv:2204.10349* .
- Lu S, Mathé P, Pereverzev SV (2020) Balancing principle in supervised learning for a general regularization scheme. *Applied and Computational Harmonic Analysis* 48(1):123–148.
- Marik PE, Linde-Zwirble WT, Bittner EA, Sahatjian J, Hansell D (2017) Fluid administration in severe sepsis and septic shock, patterns and outcomes: an analysis of a large national database. *Intensive care medicine* 43(5):625–632.
- Meister M, Steinwart I (2016) Optimal learning rates for localized svms. *The Journal of Machine Learning Research* 17(1):6722–6765.
- Moore BL, Pyeatt LD, Kulkarni V, Panousis P, Padrez K, Doufas AG (2014) Reinforcement learning for closed-loop propofol anesthesia: a study in human volunteers. *The Journal of Machine Learning Research* 15(1):655–696.
- Moore BL, Quasny TM, Doufas AG (2011) Reinforcement learning versus proportional–integral–derivative control of hypnosis in a simulated intraoperative patient. *Anesthesia & Analgesia* 112(2):350–359.
- Mücke N, Blanchard G (2018) Parallelizing spectrally regularized kernel algorithms. *The Journal of Machine Learning Research* 19(1):1069–1097.
- Murphy SA (2005a) An experimental design for the development of adaptive treatment strategies. *Statistics in medicine* 24(10):1455–1481.
- Murphy SA (2005b) A generalization error for q-learning. *Journal of Machine Learning Research* 6(Jul):1073–1097.
- Oh EJ, Qian M, Cheung YK (2022) Generalization error bounds of dynamic treatment regimes in penalized regression-based learning. *The Annals of Statistics* 50(4):2047–2071.
- Oroojlooyjadid A, Nazari M, Snyder LV, Takáč M (2022) A deep q-network for the beer game: Deep reinforcement learning for inventory optimization. *Manufacturing & Service Operations Management* 24(1):285–304.
- Padmanabhan R, Meskin N, Haddad WM (2017) Reinforcement learning-based control of drug dosing for cancer chemotherapy treatment. *Mathematical Biosciences* 293:11–20.

- Peters J, Schaal S (2008) Reinforcement learning of motor skills with policy gradients. *Neural Networks* 21(4):682–697.
- Pinelis I (1994) Optimum bounds for the distributions of martingales in banach spaces. *The Annals of Probability* 1679–1706.
- Qian M, Murphy SA (2011) Performance guarantees for individualized treatment rules. *Annals of Statistics* 39(2):1180.
- Raghu A, Komorowski M, Celi LA, Szolovits P, Ghassemi M (2017) Continuous state-space models for optimal sepsis treatment: a deep reinforcement learning approach. *Machine Learning for Healthcare Conference*, 147—163 (Boston, MA).
- Rudi A, Camoriano R, Rosasco L (2015) Less is more: Nyström computational regularization. *NIPS*, 1657–1665.
- Sabry M, Khalifa A (2019) On the reduction of variance and overestimation of deep q-learning. *arXiv preprint arXiv:1910.05983* .
- Schultz L, Sokolov V (2018) Deep reinforcement learning for dynamic urban transportation problems. *arXiv preprint arXiv:1806.05310* .
- Shi L (2019) Distributed learning with indefinite kernels. *Analysis and Applications* 17(06):947–975.
- Smale S, Zhou DX (2004) Shannon sampling and function reconstruction from point values. *Bulletin of the American Mathematical Society* 41(3):279–305.
- Smale S, Zhou DX (2005) Shannon sampling ii: Connections to learning theory. *Applied and Computational Harmonic Analysis* 19(3):285–302.
- Sugiyama M (2015) *Statistical Reinforcement Learning: Modern Machine Learning Approaches* (CRC Press).
- Sutton RS, Barto AG (2018) *Reinforcement Learning: An Introduction* (MIT press).
- Tseng HH, Luo Y, Cui S, Chien JT, Ten Haken RK, Naqa IE (2017) Deep reinforcement learning for automated radiation adaptation in lung cancer. *Medical Physics* 44(12):6690—6705.
- Tsiatis AA, Davidian M, Holloway ST, Laber EB (2019) *Dynamic Treatment Regimes: Statistical Methods for Precision Medicine* (Chapman and Hall/CRC).

-
- Vapnik V, Golowich SE, Smola AJ (1996) Support vector method for function approximation regression estimation and signal processing. *Advances in Neural Information Processing Systems 9*, 281–287 (MIT Press).
- Wahba G (1990) *Spline Models for Observational Data* (SIAM).
- Wainwright MJ (2019) Variance-reduced q-learning is minimax optimal. *arXiv preprint arXiv:1906.04697* .
- Watkins CJ, Dayan P (1992) Q-learning. *Machine Learning* 8(3-4):279–292.
- Xu X, Hu D, Lu X (2007) Kernel-based least squares policy iteration for reinforcement learning. *IEEE Transactions on Neural Networks* 18(4):973–992.
- Xu X, Xie T, Hu D, Lu X (2005) Kernel least-squares temporal difference learning. *International Journal of Information Technology* 11(9):54–63.
- Yoganarasimhan H (2020) Search personalization using machine learning. *Management Science* 66(3):1045–1070.
- Yu C, Liu J, Nemati S, Yin G (2021) Reinforcement learning in healthcare: A survey. *ACM Computing Surveys (CSUR)* 55(1):1–36.
- Zhang Y, Duchi J, Wainwright M (2015) Divide and conquer kernel ridge regression: A distributed algorithm with minimax optimal rates. *The Journal of Machine Learning Research* 16(1):3299–3340.
- Zhao X, Zhang L, Xia L, Ding Z, Yin D, Tang J (2017) Deep reinforcement learning for list-wise recommendations. *arXiv preprint arXiv:1801.00209* .
- Zhao Y, Kosorok MR, Zeng D (2009) Reinforcement learning design for cancer clinical trials. *Statistics in Medicine* 28(26):3294–3315.
- Zhao Y, Zeng D, Socinski MA, Kosorok MR (2011) Reinforcement learning strategies for clinical trials in nonsmall cell lung cancer. *Biometrics* 67(4):1422–1433.

Appendix A: Proofs

This appendix validates our main theoretical results. In the proof, we develop a novel integral operator approach for Q-learning. Our main tools are error decomposition for KRR-DTR and DKRR-DTR based on their operator representations and uniform bounds for KRR-DTR and DKRR-DTR estimators.

A.1. Operator representations and differences

The core of the integral operator approach developed in (Smale and Zhou 2005, Caponnetto and De Vito 2007), and (Lin et al. 2017) is the operator representation of kernel-based learning algorithms, error decomposition, and tight bounds of operator differences.

For each $t = 1, \dots, T$, let $S_{D,t} : \mathcal{H}_{K,t} \rightarrow \mathbb{R}^{|D|}$ be the sampling operator defined by $S_{D,t}Q_t := (Q_t(x_{i,t}))_{i=1}^{|D|}$. Its scaled adjoint $S_{D,t}^T : \mathbb{R}^{|D|} \rightarrow \mathcal{H}_{K,t}$ is given by $S_{D,t}^T \mathbf{c} := \frac{1}{|D|} \sum_{i=1}^{|D|} c_i K_{x_{i,t}}$ for $K_x = K(x, \cdot)$ and $\mathbf{c} := (c_1, c_2, \dots, c_{|D|})^T \in \mathbb{R}^{|D|}$. Define

$$L_{K,D,t}Q_t := S_{D,t}^T S_{D,t}Q_t = \frac{1}{|D|} \sum_{i=1}^{|D|} Q_t(x_{i,t}) K_{x_{i,t}}.$$

Then, $Q_{D,\lambda_t,t}$, defined by (9), can be analytically represented as (Smale and Zhou 2005)

$$Q_{D,\lambda_t,t} = (L_{K,D,t} + \lambda_t I)^{-1} S_{D,t}^T \mathbf{y}_{D,t}, \quad (29)$$

where $\mathbf{y}_{D,\lambda_t,t} := (y_{1,t}, \dots, y_{|D|,t})^T$.

Define

$$\hat{Q}_{D,\lambda_t,t} := (L_{K,D,t} + \lambda_t I)^{-1} S_{D,t}^T \mathbf{y}_{D,t}^*, \quad Q_{D,\lambda_t,t}^\circ := (L_{K,D,t} + \lambda_t I)^{-1} L_{K,D,t} Q_t^*, \quad (30)$$

where $\mathbf{y}_{D,t}^* = (y_{1,t}^*, \dots, y_{|D|,t}^*)^T$. Then $\hat{Q}_{D,\lambda_t,t}$ can be regarded as running KRR on the data set $\{(x_{i,t}, y_{i,t}^*)\}_{i=1}^{|D|}$, while $Q_{D,\lambda_t,t}^\circ$ is a noise-free version of $\hat{Q}_{D,\lambda_t,t}$. Let

$$\hat{Q}_{D_j,\lambda_t,t} := (L_{K,D_j,t} + \lambda_t I)^{-1} S_{D_j,t}^T \mathbf{y}_{D_j,t}^*, \quad Q_{D_j,\lambda_t,t}^\circ := (L_{K,D_j,t} + \lambda_t I)^{-1} L_{K,D_j,t} Q_t^* \quad (31)$$

be the corresponding local estimators for $\hat{Q}_{D,\lambda_t,t}$ and $Q_{D,\lambda_t,t}^\circ$, respectively. Define further

$$Q_{D,\lambda_t,t}^\oplus = (L_{K,t} + \lambda_t I)^{-1} S_{D,t}^T \bar{\mathbf{y}}_t \quad (32)$$

as the batch version of $Q_{D,\lambda_t,t}$, where $\bar{\mathbf{y}}_t = (\bar{y}_{1,t}, \dots, \bar{y}_{|D|,t})^T$ with

$$\bar{y}_{i,t} := r_{i,t} + \max_{a_{t+1} \in \mathcal{A}_t} \bar{Q}_{D,\lambda_{t+1},t+1}(s_{i,1:t+1}, a_{i,1:t}, a_{t+1}). \quad (33)$$

It is obvious that $Q_{D,\lambda_t,t}^\oplus$ is different from $Q_{D,\lambda_t,t}$ due to their different outputs of data. Denote

$$Q_{D,\lambda_t,t}^* := E[Y_{i,t}|X_t = x_{i,t}] = E[R(X_t, S_{T+1}) + \max_{a_{t+1}} Q_{D,\lambda_{t+1},t+1}(X_t, S_{T+1}, a_{t+1})|X_t = x_{i,t}], \quad (34)$$

and

$$\bar{Q}_{D,\lambda_t,t}^* := E[\bar{Y}_t|X_t = x_{i,t}] = E[R(X_t, S_{T+1}) + \max_{a_{t+1}} \bar{Q}_{D,\lambda_{t+1},t+1}(X_t, S_{T+1}, a_{t+1})|X_t = x_{i,t}]. \quad (35)$$

The basic idea of our analysis is to develop novel error decomposition strategies to divide $\|Q_{D,\lambda_t,t} - Q_t^*\|_{\mathcal{L}_t^2}$ into differences among $Q_{D,\lambda_t,t}$, $Q_{D,\lambda_t,t}^\oplus$, $\hat{Q}_{D,\lambda_t,t}$, $Q_{D,\lambda_t,t}^\circ$ and $\bar{Q}_{D,\lambda_t,t}$, which can be bounded by the difference between $L_{K,D,t}$ and $L_{K,t}$. For this purpose, write

$$\mathcal{W}_{D,\lambda_t,t} := \|(L_{K,t} + \lambda_t I)^{-1/2}(L_{K,t} - L_{K,D,t})(L_{K,t} + \lambda_t I)^{-1/2}\|, \quad (36)$$

$$\mathcal{A}_{D,\lambda_t,t} := \|((L_{K,t} + \lambda_t I)^{1/2}(L_{K,D,t} + \lambda_t I)^{-1}(L_{K,t} + \lambda_t I)^{1/2}\|, \quad (37)$$

$$\mathcal{U}_{D,\lambda_t,t,f} := \|(L_{K,t} + \lambda_t I)^{-1/2}(L_{K,t} - L_{K,D,t})f\|_{K,t}, \quad (38)$$

$$\mathcal{P}_{D,\lambda_t,t} := \|((L_{K,t} + \lambda_t I)^{-1/2}(S_{D,t}^T \mathbf{y}_{D,t}^* - L_{K,D,t} Q_t^*)\|_{K,t}, \quad (39)$$

$$\bar{\mathcal{S}}_{D,\lambda_t,t} := \|((L_{K,t} + \lambda_t I)^{-1/2}(S_{D,t}^T(\mathbf{y}_{D,t}^* - \bar{\mathbf{y}}_{D,t}) - L_{K,D,t}(Q_t^* - \bar{Q}_{D,\lambda_t,t}^*))\|_{K,t}, \quad (40)$$

$$\mathcal{S}_{D,\lambda_t,t} := \|((L_{K,t} + \lambda_t I)^{-1/2}(S_{D,t}^T(\mathbf{y}_{D,t}^* - \mathbf{y}_{t,\lambda_t,D}) - L_{K,D,t}(Q_t^* - Q_{D,\lambda_t,t}^*))\|_{K,t}. \quad (41)$$

Our road-map of proofs is to first decompose the generalization error into differences among $Q_{D,\lambda_t,t}$, $Q_{D,\lambda_t,t}^\oplus$, $\hat{Q}_{D,\lambda_t,t}$, $Q_{D,\lambda_t,t}^\circ$, and $\bar{Q}_{D,\lambda_t,t}$, and then quantify the differences via the above six terms, and finally derive tight estimates of these terms via some statistical tools.

A.2. Error decomposition for KRR-DTR

In this subsection, we present an error decomposition and then derive an oracle inequality for KRR-DTR.

Due to the triangle inequality, we get the following error decomposition directly.

PROPOSITION 1. *For any $1 \leq t \leq T$, we have*

$$\begin{aligned} & \|(L_{K,t} + \lambda_t I)^{1/2}(Q_{D,\lambda_t,t} - Q_t^*)\|_{K,t} \leq \|(L_{K,t} + \lambda_t I)^{1/2}(Q_{D,\lambda_t,t}^\circ - Q_t^*)\|_{K,t} \\ & + \|(L_{K,t} + \lambda_t I)^{1/2}(Q_{D,\lambda_t,t}^\circ - \hat{Q}_{D,\lambda_t,t})\|_{K,t} + \|(L_{K,t} + \lambda_t I)^{1/2}(Q_{D,\lambda_t,t} - \hat{Q}_{D,\lambda_t,t})\|_{K,t}. \end{aligned} \quad (42)$$

We call the three terms on the right-hand side of (42) as the approximation error, sample error, and multi-stage error, respectively. The approximation error, together with some regularity of the optimal Q-functions, describes the approximation capability of the RKHS $\mathcal{H}_{K,t}$. The sample error quantifies the gap between KRR

with the theoretically optimal outputs Q_t^* and KRR with noisy optimal outputs y_t^* . The multi-stage error, exclusive to Q-learning, shows the difficulty of Q-learning in circumventing its multi-stage nature. The bounds of approximation error and sample error are standard and can be derived via the recently developed integral operator approach in (Blanchard and Krämer 2016, Guo et al. 2017, Lin et al. 2020).

LEMMA 1. *Under Assumption 4 with $\frac{1}{2} \leq r \leq 1$, we have*

$$\|(L_{K,t} + \lambda_t I)^{1/2}(Q_{D,\lambda_t,t}^\circ - Q_t^*)\|_{K,t} \leq \lambda_t^r \mathcal{A}_{D,\lambda_t,t} \|h_t\|_{\mathcal{L}_t^2}, \quad \forall t = 1, \dots, T. \quad (43)$$

Proof. For any $t = 1, \dots, T$, (30) implies

$$Q_{D,\lambda_t,t}^\circ - Q_t^* = ((L_{K,D,t} + \lambda_t I)^{-1} L_{K,D,t} - I) Q_t^* = \lambda_t (L_{K,D,t} + \lambda_t I)^{-1} Q_t^*.$$

Then it follows from (37), Assumption 4, $\|Af\|_K \leq \|A\| \|f\|_K$ for positive operator A , and the fact $\|L_{K,t}^{1/2} f\|_{K,t} = \|f\|_{\mathcal{L}_t^2}$ that

$$\begin{aligned} & \|(L_{K,t} + \lambda_t I)^{1/2}(Q_{D,\lambda_t,t}^\circ - Q_t^*)\|_{K,t} \\ & \leq \lambda_t \|(L_{K,t} + \lambda_t I)^{1/2} (L_{K,D,t} + \lambda_t I)^{-1} (L_{K,t} + \lambda_t I)^{r-1/2}\| \|L_{K,t}^{1/2} h_t\|_K \\ & \leq \lambda_t^r \|(L_{K,t} + \lambda_t I)^{1/2} (L_{K,D,t} + \lambda_t I)^{-1} (L_{K,t} + \lambda_t I)^{1/2}\| \|h_t\|_{\mathcal{L}_t^2} \leq \lambda_t^r \mathcal{A}_{D,\lambda_t,t} \|h_t\|_{\mathcal{L}_t^2}. \end{aligned}$$

This completes the proof of Lemma 1. \square

LEMMA 2. *For any $t = 1, \dots, T$, it holds that*

$$\|(L_{K,t} + \lambda_t I)^{1/2}(Q_{D,\lambda_t,t}^\circ - \hat{Q}_{D,\lambda_t,t})\|_{K,t} \leq \mathcal{A}_{D,\lambda_t,t} \mathcal{P}_{D,\lambda_t,t}. \quad (44)$$

Proof. For any $t = 1, \dots, T$, it follows from (30) that

$$\hat{Q}_{D,\lambda_t,t} - Q_{D,\lambda_t,t}^\circ = (L_{K,D,t} + \lambda_t I)^{-1} (S_{D,t}^T \mathbf{y}_{D,t}^* - L_{K,D,t} Q_t^*).$$

Then, (39), (37), $\|Af\|_K \leq \|A\| \|f\|_K$ for positive operator A , and the fact $\|L_{K,t}^{1/2} f\|_{K,t} = \|f\|_{\mathcal{L}_t^2}$ yield

$$\begin{aligned} & \|(L_{K,t} + \lambda_t I)^{1/2}(Q_{D,\lambda_t,t}^\circ - \hat{Q}_{D,\lambda_t,t})\|_{K,t} \\ & \leq \|(L_{K,t} + \lambda_t I)^{1/2} (L_{K,D,t} + \lambda_t I)^{-1} (L_{K,t} + \lambda_t I)^{1/2}\| \|(L_{K,t} + \lambda_t I)^{-1/2} (S_{D,t}^T \mathbf{y}_{D,t}^* - L_{K,D,t} Q_t^*)\|_K \\ & \leq \mathcal{A}_{D,\lambda_t,t} \mathcal{P}_{D,\lambda_t,t}. \end{aligned}$$

This completes the proof of Lemma 2. \square

The bounding of the multi-stage error is more sophisticated, as collected in the following lemma.

LEMMA 3. Under Assumption 2, for any $t = 1, \dots, T$, it holds that

$$\begin{aligned} & \|(L_{K,t} + \lambda_t I)^{1/2} (Q_{D,\lambda_t,t} - \hat{Q}_{D,\lambda_t,t})\|_{K,t} \\ & \leq \mathcal{A}_{D,\lambda_t,t} \mathcal{S}_{D,\lambda_t,t} + \mathcal{A}_{D,\lambda_t,t} \mathcal{U}_{D,\lambda_t,t, Q_t^* - Q_{D,\lambda_t,t}^*}^* + \mu^{1/2} \mathcal{A}_{D,\lambda_t,t} \|Q_{D,\lambda_{t+1},t+1} - Q_{t+1}^*\|_{\mathcal{L}_{t+1}^2}. \end{aligned} \quad (45)$$

Proof. Due to (29) and (30), we have

$$\begin{aligned} & \|(L_{K,t} + \lambda_t I)^{1/2} (Q_{D,\lambda_t,t} - \hat{Q}_{D,\lambda_t,t})\|_{K,t} = \left\| (L_{K,t} + \lambda I)^{1/2} ((L_{K,D,t} + \lambda_t I)^{-1} S_{D,t}^T (\mathbf{y}_{D,t}^* - \mathbf{y}_{D,t})) \right\|_{K,t} \\ & \leq \left\| (L_{K,t} + \lambda I)^{1/2} ((L_{K,D,t} + \lambda_t I)^{-1} (S_{D,t}^T (\mathbf{y}_{D,t}^* - \mathbf{y}_{D,t}) - L_{K,D,t} (Q_t^* - Q_{D,\lambda_t,t}^*))) \right\|_{K,t} \\ & + \left\| (L_{K,t} + \lambda I)^{1/2} (L_{K,D,t} + \lambda_t I)^{-1} (L_{K,D,t} - L_{K,t}) (Q_t^* - Q_{D,\lambda_t,t}^*) \right\|_{K,t} \\ & + \left\| (L_{K,t} + \lambda I)^{1/2} (L_{K,D,t} + \lambda_t I)^{-1} L_{K,t} (Q_t^* - Q_{D,\lambda_t,t}^*) \right\|_{K,t}. \end{aligned} \quad (46)$$

It then follows from (37) and (41) that

$$\|(L_{K,t} + \lambda I)^{1/2} ((L_{K,D,t} + \lambda_t I)^{-1} (S_{D,t}^T (\mathbf{y}_{D,t}^* - \mathbf{y}_{D,t}) - L_{K,D,t} (Q_t^* - Q_{D,\lambda_t,t}^*)))\|_{K,t} \leq \mathcal{A}_{D,\lambda_t,t} \mathcal{S}_{D,\lambda_t,t}. \quad (47)$$

Furthermore, (37) and (38) yield

$$\left\| (L_{K,t} + \lambda I)^{1/2} (L_{K,D,t} + \lambda_t I)^{-1} (L_{K,D,t} - L_{K,t}) (Q_t^* - Q_{D,\lambda_t,t}^*) \right\|_{K,t} \leq \mathcal{A}_{D,\lambda_t,t} \mathcal{U}_{D,\lambda_t,t, Q_t^* - Q_{D,\lambda_t,t}^*}^*. \quad (48)$$

To bound the last term in (46), we notice

$$\begin{aligned} & \left\| (L_{K,t} + \lambda I)^{1/2} (L_{K,D,t} + \lambda_t I)^{-1} L_{K,t} (Q_t^* - Q_{D,\lambda_t,t}^*) \right\|_{K,t} \leq \mathcal{A}_{D,\lambda_t,t} \|L_{K,t}^{1/2} (Q_t^* - Q_{D,\lambda_t,t}^*)\|_{K,t} \\ & = \mathcal{A}_{D,\lambda_t,t} \|Q_t^* - Q_{D,\lambda_t,t}^*\|_{\mathcal{L}_t^2}. \end{aligned}$$

But Assumption 2, (4), (34), and (16) show

$$\begin{aligned} & \|Q_t^* - Q_{D,\lambda_t,t}^*\|_{\mathcal{L}_t^2}^2 = E \left[(Q_{D,\lambda_t,t}^*(X_t) - Q_t^*(X_t))^2 | D \right] \\ & = E \left[\left(\max_{a_{t+1}} Q_{D,\lambda_{t+1},t+1}(S_{1:t+1}, A_{1:t}, a_{t+1}) - \max_{a_{t+1}} Q_{t+1}^*(S_{1:t+1}, A_{1:t}, a_{t+1}) \right)^2 | D \right] \\ & \leq E \left[\max_{a_{t+1}} (Q_{D,\lambda_{t+1},t+1}(S_{1:t+1}, A_{1:t}, a_{t+1}) - Q_{t+1}^*(S_{1:t+1}, A_{1:t}, a_{t+1}))^2 | D \right] \\ & \leq E \left[\mu \sum_{a \in \mathcal{A}_{t+1}} (Q_{D,\lambda_{t+1},t+1}(S_{1:t+1}, A_{1:t}, a) - Q_{t+1}^*(S_{1:t+1}, A_{1:t}, a))^2 p_t(a | S_{1:t+1}, A_{1:t}) | D \right] \\ & = \mu E \left[(Q_{D,\lambda_{t+1},t+1} - Q_{t+1}^*)^2 | D \right] = \mu \|Q_{D,\lambda_{t+1},t+1} - Q_{t+1}^*\|_{L_{t+1}^2}^2. \end{aligned}$$

Therefore,

$$\left\| (L_{K,t} + \lambda I)^{1/2} (L_{K,D,t} + \lambda_t I)^{-1} L_{K,t} (Q_t^* - Q_{D,\lambda_t,t}^*) \right\|_{K,t} \leq \mu^{1/2} \mathcal{A}_{D,\lambda_t,t} \|Q_{D,\lambda_{t+1},t+1} - Q_{t+1}^*\|_{L_{t+1}^2}. \quad (49)$$

Plugging (47), (48), (49) into (46), we obtain (45) directly. This finishes the proof of Lemma 3. \square

Using Proposition 1, Lemma 1, Lemma 2 and Lemma 3, we can derive the following oracle inequality for KRR-DTR.

PROPOSITION 2. *Under Assumption 2 and Assumption 4 with $\frac{1}{2} \leq r \leq 1$, we have*

$$\begin{aligned} & \|(L_{K,t} + \lambda_t I)^{1/2}(Q_{D,\lambda_t,t} - Q_t^*)\|_{K,t} \\ & \leq \sum_{\ell=t}^T \left(\mu^{\frac{1}{2}} \mathcal{A}_{D,\lambda_\ell,\ell} \right)^{\ell-t} \mathcal{A}_{D,\lambda_\ell,\ell} \left(\lambda_t^r \|h_t\|_{\mathcal{L}_t^2} + \mathcal{P}_{D,\lambda_\ell,\ell} + \mathcal{S}_{D,\lambda_\ell,\ell} + \mathcal{U}_{D,\lambda_\ell,\ell,Q_\ell^* - Q_{D,\lambda_\ell,\ell}^*} \right). \end{aligned}$$

Proof. Inserting (43), (44) and (45) into (42), we obtain for any $t = 1, 2, \dots, T$,

$$\begin{aligned} & \|(L_{K,t} + \lambda_t I)^{1/2}(Q_{D,\lambda_t,t} - Q_t^*)\|_{K,t} \\ & \leq \mathcal{A}_{D,\lambda_t,t} \left(\lambda_t^r \|h_t\|_{\mathcal{L}_t^2} + \mathcal{P}_{D,\lambda_t,t} + \mathcal{S}_{D,\lambda_t,t} + \mathcal{U}_{D,\lambda_t,t,Q_t^* - Q_{D,\lambda_t,t}^*} \right) + \mu^{\frac{1}{2}} \mathcal{A}_{D,\lambda_t,t} \|Q_{D,\lambda_{t+1},t+1} - Q_{t+1}^*\|_{\mathcal{L}_{t+1}^2}. \end{aligned}$$

It then follows from $Q_{D,\lambda_{T+1},T+1} = Q_{T+1}^* = 0$ that

$$\begin{aligned} & \|(L_{K,t} + \lambda_t I)^{1/2}(Q_{D,\lambda_t,t} - Q_t^*)\|_{\mathcal{L}_t^2} \\ & \leq \sum_{\ell=t}^T \left(\mu^{\frac{1}{2}} \mathcal{A}_{D,\lambda_\ell,\ell} \right)^{\ell-t} \mathcal{A}_{D,\lambda_\ell,\ell} \left(\lambda_t^r \|h_t\|_{\mathcal{L}_t^2} + \mathcal{P}_{D,\lambda_\ell,\ell} + \mathcal{S}_{D,\lambda_\ell,\ell} + \mathcal{U}_{D,\lambda_\ell,\ell,Q_\ell^* - Q_{D,\lambda_\ell,\ell}^*} \right). \end{aligned}$$

Then the proof of Proposition 2 is completed. \square

A.3. Error decomposition for DKRR-DTR

The generalization error of DKRR-DTR also requires an error decomposition, as shown in the following proposition.

PROPOSITION 3. *For any $1 \leq t \leq T$, it holds that*

$$\begin{aligned} & \|(L_{K,t} + \lambda_t I)^{1/2}(\bar{Q}_{D,\lambda_t,t} - Q_t^*)\|_{K,t} \\ & \leq \sum_{j=1}^m \frac{|D_j|}{|D|} \mathcal{W}_{D_j,\lambda_t,t} \|(L_{K,t} + \lambda_t I)^{1/2}(Q_{D_j,\lambda_t,t} - Q_t^*)\|_{K,t} + \mathcal{U}_{D,\lambda_t,t,Q_t^*} + \|Q_{D,\lambda_t,t}^\oplus - Q_t^*\|_{\mathcal{L}_t^2}. \end{aligned}$$

Proof. Similar to (29), it follows from (13) and (14) that

$$\bar{Q}_{D,\lambda_t,t} = \sum_{j=1}^m \frac{|D_j|}{|D|} (L_{K,D_j,t} + \lambda_t I)^{-1} S_{D_j,t}^T \bar{\mathbf{y}}_{j,t},$$

where $\bar{\mathbf{y}}_{j,t} := (\bar{y}_{1,j,t}, \dots, \bar{y}_{|D_j|,j,t})^T$. Then

$$\begin{aligned} & \|(L_{K,t} + \lambda_t I)^{1/2}(\bar{Q}_{D,\lambda_t,t} - Q_t^*)\|_{K,t} \\ & \leq \left\| (L_{K,t} + \lambda_t I)^{1/2} \sum_{j=1}^m \frac{|D_j|}{|D|} \left((L_{K,D_j,t} + \lambda_t I)^{-1} - (L_{K,t} + \lambda_t I)^{-1} \right) S_{D_j,t}^T \bar{\mathbf{y}}_{j,t} \right\|_{K,t} \\ & \quad + \left\| (L_{K,t} + \lambda_t I)^{1/2} \sum_{j=1}^m \frac{|D_j|}{|D|} (L_{K,t} + \lambda_t I)^{-1} S_{D_j,t}^T \bar{\mathbf{y}}_{j,t} - Q_t^* \right\|_{K,t}. \end{aligned}$$

But

$$\begin{aligned} & ((L_{K,D_j,t} + \lambda_t I)^{-1} - (L_{K,t} + \lambda_t I)^{-1}) S_{D_j,t}^T \bar{\mathbf{y}}_{j,t} = (L_{K,t} + \lambda_t I)^{-1} (L_{K,t} - L_{K,D_j,t}) Q_{D_j,\lambda_t,t} \\ & = (L_{K,t} + \lambda_t I)^{-1} (L_{K,t} - L_{K,D_j,t}) (Q_{D_j,\lambda_t,t} - Q_t^*) + (L_{K,t} + \lambda_t I)^{-1} (L_{K,t} - L_{K,D_j,t}) Q_t^*, \\ & \sum_{j=1}^m \frac{|D_j|}{|D|} (L_{K,t} + \lambda_t I)^{-1} S_{D_j,t}^T \bar{\mathbf{y}}_{j,t} = (L_{K,t} + \lambda_t I)^{-1} S_{D,t}^T \bar{\mathbf{y}}_t, \end{aligned}$$

and

$$\sum_{j=1}^m \frac{|D_j|}{|D|} (L_{K,t} + \lambda_t I)^{-1} (L_{K,t} - L_{K,D_j,t}) Q_t^* = (L_{K,t} + \lambda_t I)^{-1} (L_{K,t} - L_{K,D,t}) Q_t^*.$$

Therefore, Jensen's inequality together with (32) yields

$$\begin{aligned} & \|(L_{K,t} + \lambda_t I)^{1/2} (\bar{Q}_{D,\lambda_t,t} - Q_t^*)\|_{K,t} \leq \left\| \sum_{j=1}^m \frac{|D_j|}{|D|} (L_{K,t} + \lambda_t I)^{-1/2} (L_{K,t} - L_{K,D_j,t}) (Q_{D_j,\lambda_t,t} - Q_t^*) \right\|_{\mathcal{L}_t^2} \\ & + \|(L_{K,t} + \lambda_t I)^{-1/2} (L_{K,t} - L_{K,D,t}) Q_t^*\|_{\mathcal{L}_t^2} + \|(L_{K,t} + \lambda_t I)^{1/2} (Q_{D,\lambda_t,t}^\oplus - Q_t^*)\|_{K,t} \\ & \leq \sum_{j=1}^m \frac{|D_j|}{|D|} \mathcal{W}_{D_j,\lambda_t,t} \|(L_{K,t} + \lambda_t I)^{1/2} (Q_{D_j,\lambda_t,t} - Q_t^*)\|_{K,t} + \mathcal{U}_{D,\lambda_t,t,Q_t^*} + \|(L_{K,t} + \lambda_t I)^{1/2} (Q_{D,\lambda_t,t}^\oplus - Q_t^*)\|_{K,t}. \end{aligned}$$

This completes the proof of Proposition 3. \square

Our following lemma presents an upper bound of $\|(L_{K,t} + \lambda_t I)^{1/2} (Q_{D,\lambda_t,t}^\oplus - Q_t^*)\|_{K,t}$.

LEMMA 4. *Under Assumption 2 and Assumption 4 with $\frac{1}{2} \leq r \leq 1$, for any $t = 1, \dots, T$, it holds that*

$$\begin{aligned} & \|(L_{K,t} + \lambda_t I)^{1/2} (Q_{D,\lambda_t,t}^\oplus - Q_t^*)\|_{K,t} \\ & \leq \mathcal{A}_{D,\lambda_t,t} \left(\lambda_t^r \|h_t\|_{\mathcal{L}_t^2} + \mathcal{P}_{D,\lambda_t,t} + \bar{\mathcal{S}}_{D,\lambda_t,t} + \mathcal{U}_{D,\lambda_t,t,Q_t^* - \bar{Q}_{D,\lambda_t,t}^*} \right) + \mu^{1/2} \mathcal{A}_{D,\lambda_t,t} \|\bar{Q}_{D,\lambda_{t+1},t+1} - Q_{t+1}^*\|_{L_{t+1}^2}. \end{aligned}$$

Proof. The proof of the lemma is almost the same as that in bounding $\|(L_{K,t} + \lambda_t I)^{1/2} (Q_{D,\lambda_t,t} - Q_t^*)\|_{K,t}$ in the previous subsection. For the sake of completeness, we sketch the proof. Due to the triangle inequality, it holds that

$$\begin{aligned} & \|(L_{K,t} + \lambda_t I)^{1/2} (Q_{D,\lambda_t,t}^\oplus - Q_t^*)\|_{K,t} \leq \|(L_{K,t} + \lambda_t I)^{1/2} (Q_{D,\lambda_t,t}^\circ - Q_t^*)\|_{K,t} \\ & + \|(L_{K,t} + \lambda_t I)^{1/2} (Q_{D,\lambda_t,t}^\circ - \hat{Q}_{D,\lambda_t,t})\|_{K,t} + \|(L_{K,t} + \lambda_t I)^{1/2} (Q_{D,\lambda_t,t}^\oplus - \hat{Q}_{D,\lambda_t,t})\|_{K,t}. \end{aligned}$$

Then, it follows from Lemma 1 and Lemma 2 that

$$\begin{aligned} & \|(L_{K,t} + \lambda_t I)^{1/2} (Q_{D,\lambda_t,t}^\oplus - Q_t^*)\|_{K,t} \leq \lambda_t^r \mathcal{A}_{D,\lambda_t,t} \|h_t\|_{\mathcal{L}_t^2} + \mathcal{A}_{D,\lambda_t,t} \mathcal{P}_{D,\lambda_t,t} \\ & + \|(L_{K,t} + \lambda_t I)^{1/2} (Q_{D,\lambda_t,t}^\oplus - \hat{Q}_{D,\lambda_t,t})\|_{K,t}. \end{aligned}$$

Similar as the approach in proving Lemma 3, we obtain from (32) and (30) that

$$\begin{aligned}
& \|(L_{K,t} + \lambda_t I)^{1/2} (Q_{D,\lambda_t,t}^\oplus - \hat{Q}_{D,\lambda_t,t})\|_{K,t} \\
& \leq \left\| (L_{K,t} + \lambda I)^{1/2} ((L_{K,D,t} + \lambda_t I)^{-1} (S_{D,t}^T (\mathbf{y}_{D,t}^* - \bar{\mathbf{y}}_{t,D}) - L_{K,D,t} (Q_t^* - \bar{Q}_{D,\lambda_t,t}^*)) \right\|_{K,t} \\
& + \left\| (L_{K,t} + \lambda I)^{1/2} (L_{K,D,t} + \lambda_t I)^{-1} (L_{K,D,t} - L_{K,t}) (Q_t^* - \bar{Q}_{D,\lambda_t,t}^*) \right\|_{K,t} \\
& + \left\| (L_{K,t} + \lambda I)^{1/2} (L_{K,D,t} + \lambda_t I)^{-1} L_{K,t} (Q_t^* - \bar{Q}_{D,\lambda_t,t}^*) \right\|_{K,t} \\
& \leq \mathcal{A}_{D,\lambda_t,t} \bar{\mathcal{S}}_{D,\lambda_t,t} + \mathcal{A}_{D,\lambda_t,t} \mathcal{U}_{D,\lambda_t,t, Q_t^* - \bar{Q}_{D,\lambda_t,t}^*} + \mu^{1/2} \mathcal{A}_{D,\lambda_t,t} \|\bar{Q}_{D,\lambda_{t+1},t+1} - Q_{t+1}^*\|_{L_{t+1}^2}.
\end{aligned}$$

Therefore,

$$\begin{aligned}
& \|(L_{K,t} + \lambda_t I)^{1/2} (Q_{D,\lambda_t,t}^\oplus - Q_t^*)\|_{\mathcal{L}_t^2} \\
& \leq \mathcal{A}_{D,\lambda_t,t} \left(\lambda_t^r \|h_t\|_{\mathcal{L}_t^2} + \mathcal{P}_{D,\lambda_t,t} + \bar{\mathcal{S}}_{D,\lambda_t,t} + \mathcal{U}_{D,\lambda_t,t, Q_t^* - \bar{Q}_{D,\lambda_t,t}^*} \right) + \mu^{1/2} \mathcal{A}_{D,\lambda_t,t} \|\bar{Q}_{D,\lambda_{t+1},t+1} - Q_{t+1}^*\|_{L_{t+1}^2}.
\end{aligned}$$

This completes the proof of Lemma 4. \square

We also bound $\|(L_{K,t} + \lambda I)^{1/2} (Q_{D_j,\lambda_t,t} - Q_t^*)\|_{K,t}$ in the following lemma.

LEMMA 5. *Under Assumption 2 and Assumption 4 with $\frac{1}{2} \leq r \leq 1$, for any $t = 1, \dots, T$, it holds that*

$$\begin{aligned}
& \|(L_{K,t} + \lambda_t I)^{1/2} (Q_{D_j,\lambda_t,t} - Q_t^*)\|_{K,t} \leq \mathcal{A}_{D_j,\lambda_t,t} \left(\lambda_t^r \|h_t\|_{\mathcal{L}_t^2} + \mathcal{P}_{D_j,\lambda_t,t} + \bar{\mathcal{S}}_{D_j,\lambda_t,t} + \mathcal{U}_{D_j,\lambda_t,t, Q_t^* - \bar{Q}_{D_j,\lambda_t,t}^*} \right) \\
& + \mu^{1/2} \mathcal{A}_{D_j,\lambda_t,t} \|\bar{Q}_{D,\lambda_{t+1},t+1} - Q_{t+1}^*\|_{L_{t+1}^2}.
\end{aligned}$$

Proof. It follows from Lemma 1 and Lemma 2 with $D = D_j$ that

$$\begin{aligned}
& \|(L_{K,t} + \lambda_t I)^{1/2} (Q_{D_j,\lambda_t,t} - Q_t^*)\|_{K,t} \leq \|(L_{K,t} + \lambda_t I)^{1/2} (Q_{D_j,\lambda_t,t}^\circ - Q_t^*)\|_{K,t} \\
& + \|(L_{K,t} + \lambda_t I)^{1/2} (Q_{D_j,\lambda_t,t}^\circ - \hat{Q}_{D_j,\lambda_t,t})\|_{K,t} + \|(L_{K,t} + \lambda_t I)^{1/2} (Q_{D_j,\lambda_t,t} - \hat{Q}_{D_j,\lambda_t,t})\|_{K,t} \\
& \leq \lambda_t^r \mathcal{A}_{D_j,\lambda_t,t} \|h_t\|_{\mathcal{L}_t^2} + \mathcal{A}_{D_j,\lambda_t,t} \mathcal{P}_{D_j,\lambda_t,t} + \|(L_{K,t} + \lambda_t I)^{1/2} (Q_{D_j,\lambda_t,t} - \hat{Q}_{D_j,\lambda_t,t})\|_{K,t}.
\end{aligned}$$

But for any $t = 1, \dots, T$, we have from (13), (31), and the same method in proving Lemma 3 that

$$\begin{aligned}
& \|(L_{K,t} + \lambda_t I)^{1/2} (Q_{D_j,\lambda_t,t} - \hat{Q}_{D_j,\lambda_t,t})\|_{K,t} \\
& \leq \left\| (L_{K,t} + \lambda I)^{1/2} ((L_{K,D_j,t} + \lambda_t I)^{-1} (S_{D_j,t}^T (\mathbf{y}_{D_j,t}^* - \bar{\mathbf{y}}_{t,D_j}) - L_{K,D,t} (Q_t^* - \bar{Q}_{D_j,\lambda_t,t}^*)) \right\|_{K,t} \\
& + \left\| (L_{K,t} + \lambda I)^{1/2} (L_{K,D_j,t} + \lambda_t I)^{-1} (L_{K,D_j,t} - L_{K,t}) (Q_t^* - \bar{Q}_{D_j,\lambda_t,t}^*) \right\|_{K,t} \\
& + \left\| (L_{K,t} + \lambda I)^{1/2} (L_{K,D_j,t} + \lambda_t I)^{-1} L_{K,t} (Q_t^* - \bar{Q}_{D_j,\lambda_t,t}^*) \right\|_{K,t} \\
& \leq \mathcal{A}_{D_j,\lambda_t,t} \bar{\mathcal{S}}_{D_j,\lambda_t,t} + \mathcal{A}_{D_j,\lambda_t,t} \mathcal{U}_{D_j,\lambda_t,t, Q_t^* - \bar{Q}_{D_j,\lambda_t,t}^*} + \mu^{1/2} \mathcal{A}_{D_j,\lambda_t,t} \|\bar{Q}_{D,\lambda_{t+1},t+1} - Q_{t+1}^*\|_{L_{t+1}^2}.
\end{aligned}$$

Therefore,

$$\begin{aligned} & \|(L_{K,t} + \lambda_t I)^{1/2}(Q_{D_j, \lambda_t, t} - Q_t^*)\|_{K,t} \leq \mathcal{A}_{D_j, \lambda_t, t} \left(\lambda_t^r \|h_t\|_{\mathcal{L}_t^2} + \mathcal{P}_{D_j, \lambda_t, t} + \bar{\mathcal{S}}_{D_j, \lambda_t, t} + \mathcal{U}_{D_j, \lambda_t, t, Q_t^* - \bar{Q}_{D_j, \lambda_t, t}} \right) \\ & + \mu^{-1/2} \mathcal{A}_{D_j, \lambda_t, t} \|\bar{Q}_{D, \lambda_{t+1}, t+1} - Q_{t+1}^*\|_{L_{t+1}^2}. \end{aligned}$$

This completes the proof of Lemma 5. \square

Based on Lemma 4, Lemma 5, and Proposition 3, we can derive the following oracle inequality for DKRR-DTR.

PROPOSITION 4. *Under Assumption 2 and Assumption 4 with $\frac{1}{2} \leq r \leq 1$, it holds that*

$$\begin{aligned} & \|(L_{K,t} + \lambda_t I)^{1/2}(\bar{Q}_{D, \lambda_t, t} - Q_t^*)\|_{K,t} \\ & \leq \sum_{\ell=t}^T \left(\left(\sum_{j=1}^m \frac{|D_j|}{|D|} \mathcal{W}_{D_j, \lambda_t, t} \mathcal{A}_{D_j, \lambda_t, t} + \mathcal{A}_{D, \lambda_t, t} \right) \mu^{1/2} \right)^{\ell-t} \\ & \times \left(\sum_{j=1}^m \frac{|D_j|}{|D|} \mathcal{W}_{D_j, \lambda_{\ell}, \ell} \mathcal{A}_{D_j, \lambda_{\ell}, \ell} \left(\lambda_{\ell}^r \|h_{\ell}\|_{\mathcal{L}_{\ell}^2} + \mathcal{P}_{D_j, \lambda_{\ell}, \ell} + \bar{\mathcal{S}}_{D_j, \lambda_{\ell}, \ell} + \mathcal{U}_{D_j, \lambda_{\ell}, \ell, Q_{\ell}^* - \bar{Q}_{D_j, \lambda_{\ell}, \ell}} \right) \right. \\ & \left. + \mathcal{A}_{D, \lambda_{\ell}, \ell} \left(\lambda_{\ell}^r \|h_{\ell}\|_{\mathcal{L}_{\ell}^2} + \mathcal{P}_{D, \lambda_{\ell}, \ell} + \bar{\mathcal{S}}_{D, \lambda_{\ell}, \ell} + \mathcal{U}_{D, \lambda_{\ell}, \ell, Q_{\ell}^* - \bar{Q}_{D, \lambda_{\ell}, \ell}} \right) + \mathcal{U}_{D, \lambda_{\ell}, \ell, Q_{\ell}^*} \right). \end{aligned}$$

Proof. Inserting Lemma 4 and Lemma 5 into Proposition 3, we obtain

$$\begin{aligned} & \|(L_{K,t} + \lambda_t I)^{1/2}(\bar{Q}_{D, \lambda_t, t} - Q_t^*)\|_{K,t} \\ & \leq \sum_{j=1}^m \frac{|D_j|}{|D|} \mathcal{W}_{D_j, \lambda_t, t} \mathcal{A}_{D_j, \lambda_t, t} \left(\lambda_t^r \|h_t\|_{\mathcal{L}_t^2} + \mathcal{P}_{D_j, \lambda_t, t} + \bar{\mathcal{S}}_{D_j, \lambda_t, t} + \mathcal{U}_{D_j, \lambda_t, t, Q_t^* - \bar{Q}_{D_j, \lambda_t, t}} \right) \\ & + \mathcal{A}_{D, \lambda_t, t} \left(\lambda_t^r \|h_t\|_{\mathcal{L}_t^2} + \mathcal{P}_{D, \lambda_t, t} + \bar{\mathcal{S}}_{D, \lambda_t, t} + \mathcal{U}_{D, \lambda_t, t, Q_t^* - \bar{Q}_{D, \lambda_t, t}} \right) + \mathcal{U}_{D, \lambda_t, t, Q_t^*} \\ & + \left(\sum_{j=1}^m \frac{|D_j|}{|D|} \mathcal{W}_{D_j, \lambda_t, t} \mathcal{A}_{D_j, \lambda_t, t} + \mathcal{A}_{D, \lambda_t, t} \right) \mu^{1/2} \|\bar{Q}_{D, \lambda_{t+1}, t+1} - Q_{t+1}^*\|_{L_{t+1}^2} \\ & \leq \sum_{\ell=t}^T \left(\left(\sum_{j=1}^m \frac{|D_j|}{|D|} \mathcal{W}_{D_j, \lambda_t, t} \mathcal{A}_{D_j, \lambda_t, t} + \mathcal{A}_{D, \lambda_t, t} \right) \mu^{1/2} \right)^{\ell-t} \\ & \times \left(\sum_{j=1}^m \frac{|D_j|}{|D|} \mathcal{W}_{D_j, \lambda_{\ell}, \ell} \mathcal{A}_{D_j, \lambda_{\ell}, \ell} \left(\lambda_{\ell}^r \|h_{\ell}\|_{\mathcal{L}_{\ell}^2} + \mathcal{P}_{D_j, \lambda_{\ell}, \ell} + \bar{\mathcal{S}}_{D_j, \lambda_{\ell}, \ell} + \mathcal{U}_{D_j, \lambda_{\ell}, \ell, Q_{\ell}^* - \bar{Q}_{D_j, \lambda_{\ell}, \ell}} \right) \right. \\ & \left. + \mathcal{A}_{D, \lambda_{\ell}, \ell} \left(\lambda_{\ell}^r \|h_{\ell}\|_{\mathcal{L}_{\ell}^2} + \mathcal{P}_{D, \lambda_{\ell}, \ell} + \bar{\mathcal{S}}_{D, \lambda_{\ell}, \ell} + \mathcal{U}_{D, \lambda_{\ell}, \ell, Q_{\ell}^* - \bar{Q}_{D, \lambda_{\ell}, \ell}} \right) + \mathcal{U}_{D, \lambda_{\ell}, \ell, Q_{\ell}^*} \right). \end{aligned}$$

This completes the proof of Proposition 4. \square

A.4. Bounds of operator differences

In this part, we aim to bounding the operator differences. Our first lemma focuses on bounding $\mathcal{W}_{D, \lambda_t, t}$, which can be found in (Lin et al. 2020, Lemma 6).

LEMMA 6. Let $0 < \delta \leq 1$. If Assumption 1 holds and $0 < \lambda \leq 1$, then with confidence $1 - \delta$, it holds that

$$\mathcal{W}_{D,\lambda_t,t} \leq C_1^* \mathcal{B}_{D,\lambda_t,t} \log \frac{4}{\delta}, \quad t = 1, \dots, T,$$

where $C_1^* := \max\{(\kappa^2 + 1)/3, 2\sqrt{\kappa^2 + 1}\}$ and

$$\mathcal{B}_{D,\lambda_t,t} := \frac{1 + \log(1 + \mathcal{N}_t(\lambda_t))}{\lambda|D|} + \sqrt{\frac{1 + \log(1 + \mathcal{N}_t(\lambda_t))}{\lambda|D|}}. \quad (50)$$

The second one aims to bounding $\mathcal{A}_{D,\lambda_t,t}$, which can be found in (Lin et al. 2020, Lemma 7).

LEMMA 7. If Assumption 1 holds and $0 < \lambda \leq 1$, then for $\delta \geq 4 \exp\{-1/(2C_1^* \mathcal{B}_{D,\lambda_t,t})\}$, with confidence $1 - \delta$, it holds that

$$\mathcal{A}_{D,\lambda_t,t} \leq 2, \quad t = 1, \dots, T.$$

The bound of $\mathcal{U}_{D,\lambda_t,t,f}$, provided in (Lin et al. 2017, Lemma 18), is shown in the following lemma.

LEMMA 8. Under Assumption 1, for any $0 < \delta < 1$ and $\|f\|_{L^\infty} < \infty$, with confidence at least $1 - \delta$, it holds that

$$\mathcal{U}_{D,\lambda_t,t,f} \leq \frac{2\|f\|_\infty \log(2/\delta)}{\sqrt{|D|}} \left\{ \frac{\kappa}{\sqrt{|D|\lambda_t}} + \sqrt{\mathcal{N}(\lambda_t)} \right\}, \quad t = 1, \dots, T.$$

To bound $\mathcal{P}_{D,\lambda_t,t}$, $\mathcal{S}_{D,\lambda_t,t}$ and $\bar{\mathcal{S}}_{D,\lambda_t,t}$, we should introduce a Hilbert valued Bernstein inequality established in (Pinelis 1994).

LEMMA 9. For a random variable ξ on (\mathcal{Z}, ρ) with values in a separable Hilbert space $(H, \|\cdot\|)$ satisfying $\|\xi\| \leq \bar{M} < \infty$ almost surely, and a random sample $\{z_i\}_{i=1}^s$ independent drawn according to ρ , there holds with confidence $1 - \tilde{\delta}$,

$$\left\| \frac{1}{s} \sum_{i=1}^s (\xi(z_i) - E[\xi]) \right\| \leq \frac{2\bar{M} \log(2/\tilde{\delta})}{s} + \sqrt{\frac{2E[\|\xi\|^2] \log(2/\tilde{\delta})}{s}}.$$

With the help of Lemma 9, we can derive the following concentration inequality, which is crucial to bound $\mathcal{P}_{D,\lambda_t,t}$, $\mathcal{S}_{D,\lambda_t,t}$ and $\bar{\mathcal{S}}_{D,\lambda_t,t}$.

LEMMA 10. Let $0 < \delta < 1$, $\mathbf{y}_D = (y_1, \dots, y_{|D|})^T \in \mathbb{R}^{|D|}$ with $|y_i| \leq \tilde{M}$ almost surely, and $g(x_i) = E[Y_i|x_i]$. Under Assumption 1, with confidence $1 - \delta$, it holds that

$$\|(L_{K,t} + \lambda_t I)^{-1/2} (S_{D,t} \mathbf{y}_D - L_{K,D} g)\|_{K,t} \leq \frac{2\sqrt{2}\tilde{M} \log(2/\delta)}{\sqrt{|D|}} \left(\frac{\sqrt{2}}{\sqrt{|D|\lambda_t}} + \sqrt{\mathcal{N}_t(\lambda_t)} \right).$$

Proof. Denote $z_i = (x_i, y_i)$ and $\eta_t(z_i) = (L_{K,t} + \lambda_t I)^{-1/2}(y_i - g(x_i))K_{x_i} \in \mathcal{H}_{K,t}$. Then, we have $E[\eta_t(z_i)] = 0$ and

$$\begin{aligned} \|\eta_t(z_i)\|_{K,t}^2 &= \langle (L_{K,t} + \lambda_t I)^{-1/2}(y_i - g(x_i))K_{x_i}, (L_{K,t} + \lambda_t I)^{-1/2}(y_i - g(x_i))K_{x_i} \rangle_{K,t} \\ &\leq 4\tilde{M}^2 \|(L_{K,t} + \lambda_t I)^{-1/2}(K_x)\|_{K,t}^2 = 4\tilde{M}^2 \sum_{k=1}^{\infty} \frac{(\varphi_{k,t}(x))^2}{\sigma_{k,t} + \lambda_t}, \end{aligned}$$

where $(\sigma_{k,t}, \varphi_{k,t})_{k=1}^{\infty}$ is the normalized eigen-pairs of $L_{K,t}$ in \mathcal{H}_K . Therefore, we have

$$\|\eta_t(z_i)\|_{K,t} \leq \frac{2\tilde{M}\|f\|_{L^\infty}}{\sqrt{\lambda_t}}$$

and

$$\begin{aligned} E[\|\eta_t(z_i)\|_{K,t}^2] &\leq 4\tilde{M}^2 E \left[\sum_{k=1}^{\infty} \frac{(\varphi_{k,t}(x))^2}{\sigma_{k,t} + \lambda_t} \right] = 4\tilde{M}^2 \sum_{k=1}^{\infty} \frac{E[\varphi_{k,t}^2]}{\sigma_{k,t} + \lambda_t} \\ &= 4\tilde{M}^2 \sum_{k=1}^{\infty} \frac{\sigma_{k,t}}{\sigma_{k,t} + \lambda_t} = 4\tilde{M}^2 \text{Tr}(L_{K,t}(L_{K,t} + \lambda_t I)^{-1}) = 4\tilde{M}^2 \mathcal{N}_t(\lambda_t), \end{aligned}$$

where we used the fact $E[\varphi_{k,t}^2] = \sigma_{k,t}$ which was proven in (Lin et al. 2017, eqs.(51)). Therefore, it follows from Lemma 9 that with confidence $1 - \delta$, it holds that

$$\left\| \frac{1}{|D|} \sum_{i=1}^{|D|} \eta_t(z_i) \right\| \leq \frac{4\tilde{M} \log(2/\delta)}{\sqrt{\lambda_t}|D|} + \sqrt{\frac{8\tilde{M}^2 \mathcal{N}_t(\lambda_t) \log(2/\delta)}{|D|}}.$$

This completes the proof of Lemma 10. \square

Setting $y_i = y_{i,t}^*$ and $\tilde{M} = (T - t + 1)M$ in Lemma 10, we can derive the following bound of $\mathcal{P}_{D,\lambda,t}$.

LEMMA 11. *Let $0 < \delta < 1$. Under Assumption 3, with confidence $1 - \delta$, it holds that*

$$\mathcal{P}_{D,\lambda,t} \leq \frac{2\sqrt{2}(T - t + 1)M \log(2/\delta)}{\sqrt{|D|}} \left(\frac{\sqrt{2}}{\sqrt{|D|\lambda_t}} + \sqrt{\mathcal{N}_t(\lambda_t)} \right).$$

Different from $\mathcal{P}_{D,\lambda,t}$, the bounds of $\mathcal{S}_{D,\lambda,t}$ and $\bar{\mathcal{S}}_{D,\lambda,t}$ are much more sophisticated, which requires an upper bound of $\|Q_{D,t,\lambda}\|_{\mathcal{L}_t^\infty}$ and $\|\bar{Q}_{D,t,\lambda}\|_{\mathcal{L}_t^\infty}$ for any $t = 1, \dots, T$. We leave them in the next subsection.

A.5. Uniform bounds of Q-functions

In this part, we aim at deriving $\|Q_{D,t,\lambda}\|_{\mathcal{L}_t^\infty}$ and $\|\bar{Q}_{D,t,\lambda}\|_{\mathcal{L}_t^\infty}$ so that $y_{i,t}$ and $\bar{y}_{i,t}$ can also be uniformly bounded. The following lemma presents an iterative relation between $\|Q_{D,t+1,\lambda}\|_{\mathcal{L}_{t+1}^\infty}$ and $\|Q_{D,t,\lambda}\|_{\mathcal{L}_t^\infty}$.

LEMMA 12. *Let $0 \leq \delta \leq 1$ satisfy*

$$\delta \geq 8T \exp \left\{ -\frac{2r + s}{4sC_1^*(\log(C_0 + 1) + 2)} |D|^{\frac{2r+s-1}{8r+4s}} \log^{-1} |D| \right\}. \quad (51)$$

Under Assumptions 1-5 with $\frac{1}{2} \leq r \leq 1$ and $0 < s \leq 1$, if $\lambda_t = |D|^{-\frac{1}{2r+s}}$ for $t = 1, \dots, T$, then with confidence $1 - \delta/T$, it holds that

$$\|Q_{D,\lambda_t,t}\|_{\mathcal{L}_t^\infty} + M \leq \bar{C} \sum_{\ell=t}^T (T - \ell + 2)(2\mu^{1/2})^{\ell-t} \left(\|Q_{D,\lambda_{\ell+1},\ell+1}\|_{\mathcal{L}_{\ell+1}^\infty} + M \right), \quad t = 1, 2, \dots, T, \quad (52)$$

where \bar{C} is a constant depending only on C_0, κ, r, s , and $\max_{t=1,\dots,T} \|h_t\|_{\mathcal{L}_t^2}$.

Proof. Denote $\Phi_t = \|Q_{D,\lambda_t,t}\|_{\mathcal{L}_t^\infty}$. Since $\lambda_1 = \dots = \lambda_T = |D|^{-\frac{1}{2r+s}}$, we have from Assumption 5 that

$$\mathcal{N}_t(\lambda_t) \leq C_0 \lambda_t^{-s} = C_0 |D|^{\frac{s}{2r+s}}, \quad \forall t = 1, 2, \dots, T.$$

Then

$$\frac{1}{\sqrt{|D|}} \left(\frac{1}{\sqrt{|D|\lambda_t}} + \sqrt{\mathcal{N}_t(\lambda_t)} \right) \leq (\sqrt{C_0} + 1) |D|^{\frac{-r}{2r+s}}, \quad \forall t = 1, 2, \dots, T, \quad (53)$$

and

$$\mathcal{B}_{D,\lambda_t,t} \leq \frac{2s}{2r+s} (\log(C_0 + 1) + 2) |D|^{\frac{1-2r-s}{4r+2s}} \log |D|. \quad (54)$$

Therefore, Lemma 7 and Lemma 11 yield that, with confidence $1 - \delta/(4T)$ with δ satisfying (51), there hold for any $t = 1, \dots, T$,

$$\mathcal{A}_{D,\lambda_t,t} \leq 2, \quad (55)$$

$$\mathcal{P}_{D,\lambda_t,t} \leq 4(T - t + 1)M(\sqrt{C_0} + 1) |D|^{\frac{-r}{2r+s}} \log \frac{8T}{\delta}. \quad (56)$$

We then get from Assumption 3 that $|y_{i,t}| \leq M + \Phi_{t+1}$ almost surely. Therefore, it follows from (20), Lemma (8) with $f = Q_t^* - Q_{D,\lambda_t,t}^*$, and Lemma 10 with $y_i = y_{i,t} - y_{i,t}^*$ and $\tilde{M} = (T - t + 2)M + \Phi_{t+1}$ that

$$\mathcal{U}_{D,\lambda_t,t,Q_t^*-Q_{D,\lambda_t,t}^*} \leq 2((T - t + 2)M + \Phi_{t+1})(\kappa + 1)(\sqrt{C_0} + 1) |D|^{\frac{-r}{2r+s}} \log \frac{8T}{\delta}, \quad (57)$$

$$\mathcal{S}_{D,\lambda_t,t} \leq 4((T - t + 2)M + \Phi_{t+1})(\sqrt{C_0} + 1) |D|^{\frac{-r}{2r+s}} \log \frac{8T}{\delta}, \quad (58)$$

hold with confidence $1 - \delta/(4T)$. Plugging (55), (56), (57), and (58) into Proposition 2, we obtain from (51) that

$$\begin{aligned} & \|Q_{D,\lambda_t,t} - Q_t^*\|_{K,t} \leq \lambda_t^{-1/2} \|(L_{K,t} + \lambda_t I)^{1/2} (Q_{D,\lambda_t,t} - Q_t^*)\|_{K,t} \\ & \leq \sum_{\ell=t}^T (T - t + 2)(2\mu^{1/2})^{\ell-t} (\|h_\ell\|_{\mathcal{L}_\ell^2} + (\sqrt{C_0} + 1)(M + \Phi_{\ell+1})(2\kappa + 10)) |D|^{\frac{-2r+1}{4r+2s}} \log \frac{8T}{\delta} \\ & \leq \frac{(2r+s) \sum_{\ell=t}^T (T - \ell + 2)(2\mu^{1/2})^{\ell-t} \left(\|h_\ell\|_{\mathcal{L}_\ell^2} + (\sqrt{C_0} + 1)(M + \Phi_{\ell+1})(2\kappa + 10) \right)}{(4sC_1^* (\log(C_0 + 1) + 2))} \\ & \leq \bar{C}_1 \sum_{\ell=t}^T (T - \ell + 2)(2\mu^{1/2})^{\ell-t} (\Phi_{\ell+1} + M) \end{aligned}$$

holds with confidence $1 - \delta/T$, where δ satisfies (51), and

$$\bar{C}_1 := \frac{4(2r+s) \left(\max_{\ell=1, \dots, T} \|h_\ell\|_{\mathcal{L}_\ell^2} + (\sqrt{C_0} + 1)(2\kappa + 10) \right)}{4sC_1^*(\log(C_0 + 1) + 2)}.$$

Therefore, we have

$$\begin{aligned} & \|Q_{D, \lambda_t, t}\|_{\mathcal{L}_t^\infty} + M \leq \kappa \|Q_{D, \lambda_t, t}\|_{K, t} + M \leq \kappa \|Q_{D, \lambda_t, t} - Q_t^*\|_{K, t} + \kappa \|Q_t^*\|_{K, T} + M \\ & \leq \bar{C} \sum_{\ell=t}^T (T - t + 2)(2\mu^{1/2})^{\ell-t} (\Phi_{\ell+1} + M), \end{aligned}$$

where $\bar{C} := \kappa \bar{C}_1 + \kappa^{2r} \max_{t=1, \dots, T} \|h_t\|_{\mathcal{L}_t^2} + 1$. This completes the proof of Lemma 12. \square

Based on the above lemma, we can derive an upper bound of $\|Q_{D, \lambda_t, t}\|_{\mathcal{L}_t^\infty}$.

PROPOSITION 5. *Let $0 \leq \delta \leq 1$ with δ satisfying (51). Under Assumptions 1-5 with $\frac{1}{2} \leq r \leq 1$ and $0 < s \leq 1$, if $\lambda_t = |D|^{-\frac{1}{2r+s}}$ for $t = 1, \dots, T$, then with confidence $1 - \delta$, it holds that*

$$\|Q_{D, \lambda_t, t}\|_{\mathcal{L}_t^\infty} \leq 2\bar{C}^T (2\mu^{1/2})^{T-t} M \prod_{\ell=t}^{T-1} ((T - \ell + 2)(2\mu^{1/2})^{\ell-t} + 1) - M, \quad t = 1, \dots, T.$$

Proof. Since for any $\xi_t, \eta_t > 0$, $\xi_t \leq \sum_{\ell=t}^T \eta_\ell \xi_{\ell+1}$ implies $\xi_t \leq \prod_{\ell=t}^{T-1} (\eta_\ell + 1) \eta_T \xi_{T+1}$. Set $\xi_t = \|Q_{D, \lambda_t, t}\|_{\mathcal{L}_t^\infty} + M$ and $\eta_t = \bar{C}(T - \ell + 1)(2\mu^{-1/2})^{\ell-t}$. We have from (52) and $Q_{D, \lambda_{T+1}, T+1} = 0$ that

$$\|Q_{D, \lambda_t, t}\|_{\mathcal{L}_t^\infty} + M \leq \prod_{\ell=t}^{T-1} (\bar{C}(T - \ell + 2)(2\mu^{1/2})^{\ell-t} + 1) 2\bar{C}(2\mu^{1/2})^{T-t} M.$$

This completes the proof Proposition 5. \square

Similar to Lemma 12, we present an iteration relation between $\|\bar{Q}_{D, \lambda_t, t}\|_{\mathcal{L}_t^\infty}$ and $\|\bar{Q}_{D, \lambda_{t+1}, t+1}\|_{\mathcal{L}_{t+1}^\infty}$.

LEMMA 13. *Let $0 \leq \delta \leq 1$ satisfy*

$$\delta \geq 40Tm \exp \left\{ -\frac{2r+s}{4sC_1^*(\log(C_0 + 1) + 2)} |D|^{\frac{2r+s-1}{16r+8s}} m^{-1/2} \log^{-1} |D| \right\}. \quad (59)$$

Under Assumptions 1-5 with $\frac{1}{2} \leq r \leq 1$ and $0 < s \leq 1$, if $\lambda_t = |D|^{-\frac{1}{2r+s}}$ for $t = 1, \dots, T$, $|D_1| = \dots = |D_m|$, and m satisfies (25), then with confidence $1 - \delta/T$, it holds that

$$\|Q_{D, \lambda_t, t}\|_{\mathcal{L}_t^\infty} + M \leq \hat{C} \sum_{\ell=t}^T (T - t + 2)(2\mu^{1/2})^{\ell-t} (\Phi_{\ell+1} + M), \quad t = 1, 2, \dots, T, \quad (60)$$

where \hat{C} is a constant depending only on C_0, κ, r, s , and $\max_{t=1, \dots, T} \|h_t\|_{\mathcal{L}_t^2}$.

Proof. Write $\Psi_t = \|\bar{Q}_{D, \lambda_t, t}\|_{\mathcal{L}_t^2}$. Since $|D_1| = \dots = |D_m|$ and $\lambda_1 = \dots = \lambda_T = |D|^{-\frac{1}{2r+s}}$, (25) yields

$$\frac{1}{\sqrt{|D_j|}} \left(\frac{1}{\sqrt{|D_j|} \lambda_t} + \sqrt{\mathcal{N}_t(\lambda_t)} \right) \leq (\sqrt{C_0} + 1) \sqrt{m} |D|^{\frac{-r}{2r+s}}, \quad \forall t = 1, 2, \dots, T, \quad (61)$$

and

$$\mathcal{B}_{D,\lambda_t,t} \leq \frac{2s}{2r+s} (\log(C_0+1)+2)\sqrt{m}|D|^{\frac{1-2r-s}{4r+2s}} \log|D|. \quad (62)$$

From Lemma 6, Lemma 7, and Lemma 11 with $D = D_j$, we obtain that for any δ satisfying (59), with confidence $1 - \delta/(10mT)$, it holds that

$$\mathcal{W}_{D_j,\lambda_t,t} \leq C_1^* \frac{2s}{2r+s} (\log(C_0+1)+2)\sqrt{m}|D|^{\frac{1-2r-s}{4r+2s}} \log|D| \log \frac{40mT}{\delta}, \quad (63)$$

$$\mathcal{A}_{D_j,\lambda_t,t} \leq 2, \quad (64)$$

$$\mathcal{P}_{D_j,\lambda_t,t} \leq 4(T-t+1)M(\sqrt{C_0}+1)\sqrt{m}|D|^{\frac{-r}{2r+s}} \log \frac{20mT}{\delta}. \quad (65)$$

We then get from Assumption 3 that $|\bar{y}_{i,t}| \leq M + \Psi_{t+1}$ almost surely. Therefore, it follows from (20), Lemma 8 with $f = Q_t^* - \bar{Q}_{D,\lambda_t,t}^*$, and Lemma 10 with $y_i = \bar{y}_{i,t} - y_{i,t}^*$ and $\tilde{M} = (T-t+2)M + \Psi_{t+1}$ that

$$\mathcal{U}_{D_j,\lambda_t,t,Q_t^*-\bar{Q}_{D,\lambda_t,t}^*} \leq 2((T-t+2)M + \Psi_{t+1})(\kappa+1)(\sqrt{C_0}+1)\sqrt{m}|D|^{\frac{-r}{2r+s}} \log \frac{20mT}{\delta}, \quad (66)$$

$$\bar{\mathcal{S}}_{D_j,\lambda_t,t} \leq 4((T-t+2)M + \Psi_{t+1})(\sqrt{C_0}+1)\sqrt{m}|D|^{\frac{-r}{2r+s}} \log \frac{20mT}{\delta} \quad (67)$$

hold with confidence $1 - \delta/(10mT)$. Hence, with confidence $1 - \delta/(2mT)$ with δ satisfying (59), we have from (25) that

$$\begin{aligned} & \left(\sum_{j=1}^m \frac{|D_j|}{|D|} \mathcal{W}_{D_j,\lambda_t,t} \mathcal{A}_{D_j,\lambda_t,t} + \mathcal{A}_{D,\lambda_t,t} \right)^{\ell-t} \\ & \leq \left(C_1^* \frac{2s}{2r+s} (\log(C_0+1)+2)\sqrt{m}|D|^{\frac{1-2r-s}{2r+s}} \log|D| \log \frac{40mT}{\delta} + 1 \right)^{\ell-t} \leq 2^{\ell-t} \end{aligned}$$

and

$$\begin{aligned} & \lambda_t^{-1/2} \sum_{j=1}^m \frac{|D_j|}{|D|} \mathcal{W}_{D_j,\lambda_\ell,\ell} \mathcal{A}_{D_j,\lambda_\ell,\ell} (\lambda_\ell^r \|h_\ell\|_{\mathcal{L}_\ell^2} + \mathcal{P}_{D_j,\lambda_\ell,\ell} + \bar{\mathcal{S}}_{D_j,\lambda_\ell,\ell} + \mathcal{U}_{D_j,\lambda_\ell,\ell,Q_\ell^*-\bar{Q}_{D_j,\lambda_\ell,\ell}^*}) \\ & \leq \hat{C}_1 (T-t+2)(M + \Psi_{t+1})m|D|^{\frac{1-2r-s}{4r+2s}} \log|D| |D|^{-\frac{2r-1}{4r+2s}} \log^2 \frac{40mT}{\delta} \\ & \leq 4\hat{C}_1 (T-t+2)(M + \Psi_{t+1}), \end{aligned}$$

where

$$\hat{C}_1 := \max_{t=1,\dots,T} \|h_t\|_{\mathcal{L}_t^2} + 4(\sqrt{C_0}+1) + 4(\sqrt{C_0}+1) + 2(\kappa+1)(\sqrt{C_0}+1).$$

Similarly, we can derive from (55), (56), (57), and (58) that, with confidence $1 - \delta/(2T)$ with δ satisfying (59), it holds that

$$\begin{aligned} & \lambda_t^{-1/2} \mathcal{A}_{D,\lambda_\ell,\ell} (\lambda_\ell^r \|h_\ell\|_{\mathcal{L}_\ell^2} + \mathcal{P}_{D,\lambda_\ell,\ell} + \bar{\mathcal{S}}_{D,\lambda_\ell,\ell} + \mathcal{U}_{D,\lambda_\ell,\ell,Q_\ell^*-\bar{Q}_{D,\lambda_\ell,\ell}^*}) + \mathcal{U}_{D,\lambda_\ell,\ell,Q_\ell^*} \\ & \leq \hat{C}_2 \sum_{\ell=t}^T (T-\ell+2)(2\mu^{1/2})^{\ell-t} (\Phi_{\ell+1} + M), \end{aligned}$$

where $\hat{C}_2 := \bar{C}_1 + 1$. The above three estimates together with (4) yield that, with confidence $1 - \delta/T$, it holds that

$$\begin{aligned} & \|\bar{Q}_{D,\lambda_t,t} - Q_t^*\|_{K,t} \leq \lambda_t^{-1/2} \|(L_{K,t} + \lambda_t I)^{1/2} (\bar{Q}_{D,\lambda_t,t} - Q_t^*)\|_{K,t} \\ & \leq (\hat{C}_2 + 2\hat{C}_3) \sum_{\ell=t}^T (2\mu^{1/2})^{\ell-t} \sum_{\ell=t}^T (T - \ell + 2) (2\mu^{1/2})^{\ell-t} (\Phi_{\ell+1} + M). \end{aligned}$$

Therefore, we have

$$\begin{aligned} & \|\bar{Q}_{D,\lambda_t,t}\|_{\mathcal{L}_t^\infty} + M \leq \kappa \|\bar{Q}_{D,\lambda_t,t}\|_{K,t} + M \leq \kappa \|\bar{Q}_{D,\lambda_t,t} - Q_t^*\|_{K,t} + \kappa \|Q_t^*\|_{K,T} + M \\ & \leq \hat{C} \sum_{\ell=t}^T (T - t + 2) (\hat{C}_1 \mu^{1/2})^{\ell-t} (\Phi_{\ell+1} + M), \end{aligned}$$

where $\hat{C} := \kappa(\hat{C}_1 + 2\hat{C}_2) + \kappa^{2r} \max_{t=1,\dots,T} \|h_t\|_{\mathcal{L}_t^2} + 1$. This completes the proof of Lemma 13. \square

Using the same approach as that in proving Proposition 5, we can derive the following proposition directly.

PROPOSITION 6. *Let $0 \leq \delta \leq 1$ with δ satisfying (59). Under Assumptions 1-5 with $\frac{1}{2} \leq r \leq 1$ and $0 < s \leq 1$, if $\lambda_t = |D|^{-\frac{1}{2r+s}}$ for $t = 1, \dots, T$, $|D_1| = \dots = |D_m|$, and m satisfies (25), then with confidence $1 - \delta$, it holds that*

$$\|Q_{D,\lambda_t,t}\|_{\mathcal{L}_t^\infty} \leq 2\hat{C}^T (2\mu^{1/2})^{T-t} M \prod_{\ell=t}^{T-1} ((T - \ell + 2) (2\mu^{1/2})^{\ell-t} + 1) - M, \quad t = 1, \dots, T.$$

A.6. Deriving generalization errors

In this subsection, we derive the generalization error of KRR-DTR and DKRR-DTR. To prove our main theorems, we need the following lemma, which is standard in statistical learning theory. We present its proof for the sake of completeness.

LEMMA 14. *Let $0 < \delta < 1$, and $\xi \in \mathbb{R}_+$ be a random variable. If $\xi \leq u \log^b \frac{c}{\delta}$ holds with confidence $1 - \delta$ for some $u, b, c > 0$, then*

$$E[\xi] \leq c\Gamma(b+1)u,$$

where $\Gamma(\cdot)$ is the Gamma function.

Proof. Since $\xi \leq u \log^b \frac{c}{\delta}$ holds with confidence $1 - \delta$, we have

$$P[\xi > t] \leq c \exp\{u^{-1/b} t^{1/b}\}.$$

Using the probability to expectation formula

$$E[\xi] = \int_0^\infty P[\xi > \varepsilon] d\varepsilon \tag{68}$$

to the positive random variable ξ , we have

$$E[\xi] \leq c \int_0^\infty \exp\{u^{-1/b} \varepsilon^{1/b}\} d\varepsilon \leq cu\Gamma(b+1).$$

This completes the proof of Lemma 14. \square

With the above foundations, we are in a position to prove our main theorems.

Proof of Theorem 1. It follows from Proposition 2 that

$$\begin{aligned} E[\|(Q_{D,\lambda_t,t} - Q_t^*)\|_{\mathcal{L}_t^2}] &\leq E[\|(L_{K,t} + \lambda_t I)^{1/2}(Q_{D,\lambda_t,t} - Q_t^*)\|_{K,t}] \\ &\leq \sum_{\ell=t}^T \mu^{\frac{\ell-t}{2}} E \left[\mathcal{A}_{D,\lambda_\ell,\ell}^{\ell-t+1} (\lambda_\ell^r \|h_\ell\|_{\mathcal{L}_\ell^2} + \mathcal{P}_{D,\lambda_\ell,\ell} + \mathcal{S}_{D,\lambda_\ell,\ell} + \mathcal{U}_{D,\lambda_\ell,\ell,Q_\ell^* - Q_{D,\lambda_\ell,\ell}^*}) \right]. \end{aligned}$$

For $\lambda_1 = \dots = \lambda_T = |D|^{-\frac{1}{2r+s}}$, it follows from (55), (56), (58), (57), and Proposition 5 that, with confidence $1 - \delta$ with δ satisfying (51), it holds that

$$\begin{aligned} &\mathcal{A}_{D,\lambda_\ell,\ell}^{\ell-t+1} \left(\lambda_\ell^r \|h_\ell\|_{\mathcal{L}_\ell^2} + \mathcal{P}_{D,\lambda_\ell,\ell} + \mathcal{S}_{D,\lambda_\ell,\ell} + \mathcal{U}_{D,\lambda_\ell,\ell,Q_\ell^* - Q_{D,\lambda_\ell,\ell}^*} \right) \\ &\leq 2^{\ell-t} \tilde{C}_1 \bar{C}^T (2\mu^{1/2})^{T-\ell} M \prod_{k=\ell}^{T-1} ((T-k+2)(2\mu^{1/2})^{k-\ell} + 1) |D|^{\frac{-r}{2r+s}} \log \frac{8T}{\delta}, \end{aligned}$$

where

$$\tilde{C}_1 := 4 \max_{t=1,\dots,T} \|h_t\|_{\mathcal{L}_t^2} + 16M(\sqrt{C_0} + 1) + 2(\kappa + 1)(\sqrt{C_0} + 1) + 4(\sqrt{C_0} + 1).$$

Then it follows from Lemma 14, (68), and (51) that

$$\begin{aligned} E[\|(Q_{D,\lambda_t,t} - Q_t^*)\|_{\mathcal{L}_t^2}] &\leq \int_0^\infty P[\|(Q_{D,\lambda_t,t} - Q_t^*)\|_{\mathcal{L}_t^2} > \varepsilon] d\varepsilon \\ &= \int_0^{8T} \exp\left\{-\frac{2r+s}{4sC_1^*(\log(C_0+1)+2)} |D|^{\frac{2r+s-1}{8r+4s}} \log^{-1} |D|\right\} P[\|(Q_{D,\lambda_t,t} - Q_t^*)\|_{\mathcal{L}_t^2} > \varepsilon] d\varepsilon \\ &\quad + \int_{8T}^\infty \exp\left\{-\frac{2r+s}{4sC_1^*(\log(C_0+1)+2)} |D|^{\frac{2r+s-1}{8r+4s}} \log^{-1} |D|\right\} d\varepsilon \\ &\leq 8T \exp\left\{-\frac{2r+s}{4sC_1^*(\log(C_0+1)+2)} |D|^{\frac{2r+s-1}{8r+4s}} \log^{-1} |D|\right\} + \int_0^\infty P[\|(Q_{D,\lambda_t,t} - Q_t^*)\|_{\mathcal{L}_t^2} > \varepsilon] d\varepsilon \\ &\leq \tilde{C}_2 T \sum_{\ell=t}^T \mu^{\frac{\ell-t}{2}} 2^{\ell-t} \bar{C}^T (2\mu^{1/2})^{T-\ell} \prod_{k=\ell}^{T-1} ((T-k+2)(2\mu^{1/2})^{k-\ell} + 1) |D|^{\frac{-r}{2r+s}}, \end{aligned}$$

where \tilde{C}_2 is a constant depending only on \tilde{C}_1 , M , r , s , and C_0 . Noting further (18), we then have

$$\begin{aligned} &E[V_1^*(S_1) - V_{\pi_{D,\bar{X},1}}(S_1)] \\ &\leq C_1 \sum_{t=1}^T \mu^{t/2} T \sum_{\ell=t}^T \mu^{\frac{\ell-t}{2}} 2^{\ell-t} \bar{C}^T (2\mu^{1/2})^{T-\ell} \prod_{k=\ell}^{T-1} ((T-k+2)(2\mu^{1/2})^{k-\ell} + 1) |D|^{\frac{-r}{2r+s}} \end{aligned}$$

for $C_1 = 2\tilde{C}$. This completes the proof of Theorem 1. \square

Proof of Theorem 2. It follows from Proposition 4 that

$$\begin{aligned}
& E[\|\bar{Q}_{D,\lambda_t,t} - Q_t^*\|_{\mathcal{L}_t^2}] \leq E[\|(L_{K,t} + \lambda_t I)^{1/2}(\bar{Q}_{D,\lambda_t,t} - Q_t^*)\|_{K,t}] \\
& \leq \sum_{\ell=t}^T E \left[\left(\left(\sum_{j=1}^m \frac{|D_j|}{|D|} \mathcal{W}_{D_j,\lambda_{\ell,t}} \mathcal{A}_{D_j,\lambda_{\ell,t}} + \mathcal{A}_{D,\lambda_{\ell,t}} \right) \mu^{1/2} \right)^{\ell-t} \right. \\
& \times \left(\sum_{j=1}^m \frac{|D_j|}{|D|} \mathcal{W}_{D_j,\lambda_{\ell,\ell}} \mathcal{A}_{D_j,\lambda_{\ell,\ell}} \left(\lambda_{\ell}^r \|h_{\ell}\|_{\mathcal{L}_{\ell}^2} + \mathcal{P}_{D_j,\lambda_{\ell,\ell}} + \bar{\mathcal{S}}_{D_j,\lambda_{\ell,\ell}} + \mathcal{U}_{D_j,\lambda_{\ell,\ell},Q_{\ell}^* - \bar{Q}_{D_j,\lambda_{\ell,\ell}}^*} \right) \right. \\
& \left. \left. + \mathcal{A}_{D,\lambda_{\ell,\ell}} \left(\lambda_{\ell}^r \|h_{\ell}\|_{\mathcal{L}_{\ell}^2} + \mathcal{P}_{D,\lambda_{\ell,\ell}} + \bar{\mathcal{S}}_{D,\lambda_{\ell,\ell}} + \mathcal{U}_{D,\lambda_{\ell,\ell},Q_{\ell}^* - \bar{Q}_{D,\lambda_{\ell,\ell}}^*} \right) + \mathcal{U}_{D,\lambda_{\ell,\ell},Q_{\ell}^*} \right) \right].
\end{aligned}$$

But (59), (64), (55), (25), (64), (65), (67), (66), and Proposition 6 yield that for any $t = 1, \dots, T$, with confidence $1 - \delta/2$, it holds that

$$\left(\sum_{j=1}^m \frac{|D_j|}{|D|} \mathcal{W}_{D_j,\lambda_{t,t}} \mathcal{A}_{D_j,\lambda_{t,t}} + \mathcal{A}_{D,\lambda_{t,t}} \right) \leq 2$$

and

$$\begin{aligned}
& \sum_{j=1}^m \frac{|D_j|}{|D|} \mathcal{W}_{D_j,\lambda_{\ell,\ell}} \mathcal{A}_{D_j,\lambda_{\ell,\ell}} (\lambda_{\ell}^r \|h_{\ell}\|_{\mathcal{L}_{\ell}^2} + \mathcal{P}_{D_j,\lambda_{\ell,\ell}} + \bar{\mathcal{S}}_{D_j,\lambda_{\ell,\ell}} + \mathcal{U}_{D_j,\lambda_{\ell,\ell},Q_{\ell}^* - \bar{Q}_{D_j,\lambda_{\ell,\ell}}^*}) \\
& \leq \tilde{C}_3 m |D|^{\frac{1-2r-s}{4r+2s}} \log |D| |D|^{-\frac{r}{2r+s}} \hat{C}^T (2\mu^{1/2})^{T-t} \prod_{\ell=t}^{T-1} ((T-\ell+2)(2\mu^{1/2})^{\ell-t} + 1) \log \frac{40mT}{\delta} \\
& \leq \tilde{C}_3 |D|^{-\frac{r}{2r+s}} \hat{C}^T (2\mu^{1/2})^{T-t} \prod_{\ell=t}^{T-1} ((T-\ell+2)(2\mu^{1/2})^{\ell-t} + 1) \log \frac{40}{\delta},
\end{aligned}$$

where we use $\log ab \leq (\log a + 1) \log b$ for $a, b \geq 3$ in the last inequality, and

$$\tilde{C}_3 := 6MC_1^* \frac{2s}{2r+s} (\log(C_0 + 1) + 2) \left(\max_{t=1,\dots,T} \|h_t\|_{\mathcal{L}_t^2} + 8(\sqrt{C_0} + 1) \right) + 2(\kappa + 1)(\sqrt{C_0} + 1).$$

Similarly, we can derive that with confidence $1 - \delta/2$, it holds that

$$\begin{aligned}
& \mathcal{A}_{D,\lambda_{\ell,\ell}} (\lambda_{\ell}^r \|h_{\ell}\|_{\mathcal{L}_{\ell}^2} + \mathcal{P}_{D,\lambda_{\ell,\ell}} + \bar{\mathcal{S}}_{D,\lambda_{\ell,\ell}} + \mathcal{U}_{D,\lambda_{\ell,\ell},Q_{\ell}^* - \bar{Q}_{D,\lambda_{\ell,\ell}}^*}) + \mathcal{U}_{D,\lambda_{\ell,\ell},Q_{\ell}^*} \\
& \leq \tilde{C}_4 |D|^{-\frac{r}{2r+s}} \hat{C}^T (2\mu^{1/2})^{T-t} \prod_{\ell=t}^{T-1} ((T-\ell+2)(2\mu^{1/2})^{\ell-t} + 1) \log \frac{40T}{\delta},
\end{aligned}$$

where

$$\tilde{C}_4 := 6M \left(\max_{t=1,\dots,T} \|h_t\|_{\mathcal{L}_t^2} + 8(\sqrt{C_0} + 1) \right) + 2(\kappa + 1)(\sqrt{C_0} + 1).$$

Hence, we have from Lemma 14 that

$$\begin{aligned}
& E[\|\bar{Q}_{D,\lambda_t,t} - Q_t^*\|_{\mathcal{L}_t^2}] \leq 40Tm \exp \left\{ -\frac{2r+s}{4sC_1^* (\log(C_0 + 1) + 2)} |D|^{\frac{2r+s-1}{16r+8s}} m^{-1/2} \log^{-1} |D| \right\} \\
& + 80(\tilde{C}_3 + \tilde{C}_4)T |D|^{-\frac{r}{2r+s}} \hat{C}^T (2\mu^{1/2})^{T-t} \prod_{\ell=t}^{T-1} ((T-\ell+2)(2\mu^{1/2})^{\ell-t} + 1) \\
& \leq C_2 T |D|^{-\frac{r}{2r+s}} \hat{C}^T (2\mu^{1/2})^{T-t} \prod_{\ell=t}^{T-1} ((T-\ell+2)(2\mu^{1/2})^{\ell-t} + 1),
\end{aligned}$$

where C_2 is a constant depending only on $\max_{t=1,\dots,T} \|h_t\|_{\mathcal{L}_t^2}$, C_0 , κ , M , r , and s . This together with (19) completes the proof of Theorem 2. \square

Appendix B: Algorithm of DKRR-DTK

In this section, we present the detailed implementation of DKRR-DTR as shown in Algorithm 1, where the steps above the dashed line are the implementation of the training process and the steps below the dashed line are the implementation of decision-making for a query. In Algorithm 1, $\text{Model}(s, a)$ denotes the contents of the environment model that predicts the next state and reward for state-action pair (s, a) , and it is related to the types of clinical trials.

Algorithm 1 DKRR-DTR

Input: Data subset $D_j = \{(s_{i,j,1}, a_{i,j,1}, r_{i,j,1}, \dots, s_{i,j,T}, a_{i,j,T}, r_{i,j,T}, s_{i,j,T+1})\}_{i=1}^{|D_j|}$ stored in the j -th local machine

for $j = 1, \dots, m$; families \mathcal{A}_t of actions at stage t for $t = 1, \dots, T$; a query with initial state $s_1^{(q)}$.

1: **for** $j = 1, 2, \dots, m$ **do** ▷ Initialization

2: Initialize the label vector $\vec{Y}_{D_j, T} := [\bar{y}_{1,j,T}, \dots, \bar{y}_{|D_j|,j,T}]^\top = [r_{1,j,T}, \dots, r_{|D_j|,j,T}]^\top$.

3: **end for**

4: **for** $t = T, T-1, \dots, 1$ **do** ▷ Training process

5: **for** $j = 1, 2, \dots, m$ **do** ▷ Local process

6: Run KRR on the j -th local machine with data D_j and parameter λ_t to obtain a function

$$Q_{D_j, \lambda_t, t} = \arg \min_{Q_t \in \mathcal{H}_{K,t}} \frac{1}{|D_j|} \sum_{i=1}^{|D_j|} (\bar{y}_{i,j,t} - Q_t(s_{i,j,1:t}, a_{i,j,1:t}))^2 + \lambda_t \|Q_t\|_{K,t}^2.$$

7: Communicate $\{s_{i,j,1:t}, a_{i,j,1:t-1}\}_{i=1}^{|D_j|}$ to the k -th local machine for $k = 1, \dots, m$.

8: **for** a_t in \mathcal{A}_t **do**

9: Compute m vectors

$$\vec{H}_{D_j, k, a_t, t} = [Q_{D_j, \lambda_t, t}(s_{1,k,1:t}, a_{1,k,1:t-1}, a_t), \dots, Q_{D_j, \lambda_t, t}(s_{|D_k|, k, 1:t}, a_{|D_k|, k, 1:t-1}, a_t)]^\top$$

for $k = 1, \dots, m$, and communicate these m vectors to the global machine.

10: **end for**

11: **end for**

12: **for** a_t in \mathcal{A}_t **do** ▷ Synthesization

13: Synthesize m global vectors, $\vec{H}_{D, k, a_t, t} = \sum_{j=1}^m \frac{|D_j|}{|D|} \vec{H}_{D_j, k, a_t, t}$ for $k = 1, \dots, m$.

14: Distribute m vectors $\vec{H}_{D,k,a_t,t}$ with $k = 1, \dots, m$ to each local machine.

15: **end for**

16: **for** $j = 1, 2, \dots, m$ **do** ▷ Local process

17: Compute the label vector $\vec{Y}_{D_j,t-1} = \vec{R}_{D_j,t-1} + \max_{a_t \in \mathcal{A}_t} \vec{H}_{D,j,a_t,t}$, where “max” is an element-wise operator for vectors $\vec{H}_{D,j,a_t,t}$, and $\vec{R}_{D_j,t-1} = [r_{1,j,t-1}, \dots, r_{|D_j|,j,t-1}]^\top$.

18: **end for**

19: **end for**

20: **for** $t = 1, 2, \dots, T$ **do** ▷ Decision-making

21: Distribute the query state $s_t^{(q)}$ to m local machines.

22: **for** $j = 1, 2, \dots, m$ **do** ▷ Local process

23: On the j -th local machine, compute $|\mathcal{A}_t|$ values

$$h_{D_j,a_t,t}^{(q)} = Q_{D_j,\lambda_t,t} \left(s_{1:t}^{(q)}, a_{1:t-1}^{(q)}, a_t \right)$$

 for a_t in \mathcal{A}_t , and communicate these $|\mathcal{A}_t|$ values to the global machine.

24: **end for**

25: Generate $|\mathcal{A}_t|$ global estimators, $h_{D,a_t,t}^{(q)} = \sum_{j=1}^m \frac{|D_j|}{|D|} h_{D_j,a_t,t}^{(q)}$ for a_t in \mathcal{A}_t . ▷ Synthesization

26: Take an action $a_t^{(q)} = \arg \max_{a_t \in \mathcal{A}_t} h_{D,a_t,t}^{(q)}$. ▷ Policy

27: Get the next state and reward for the state-action pair $(s_t^{(q)}, a_t^{(q)})$ according to

$$(s_{t+1}^{(q)}, r_t^{(q)}) := \text{Model} \left(s_t^{(q)}, a_t^{(q)} \right). \quad \text{▷ Environment model}$$

28: **end for**

Output: A treatment trajectory $(s_1^{(q)}, a_1^{(q)}, r_1^{(q)}, \dots, s_T^{(q)}, a_T^{(q)}, r_T^{(q)}, s_{T+1}^{(q)})$ for the query with initial state $s_1^{(q)}$.

Appendix C: Introduction of Simulation 1

This section provides a thorough description of the trajectory data production for Section 5.1. The observation period for patients in the clinical trial is 5 years. At each time point $t \in [0, 5]$, the tumor size denoted by $M(t)$ and the wellness denoted by $W(t)$ for each patient are recorded. When a patient’s wellness is less than 0.25, the patient suffers from death. When a patient’s tumor size reaches 1, that is, when a time point t_i satisfies $M(t_i) = 1$, treatment should be administered. Here, an aggressive treatment (denoted by A) or a conservative treatment (denoted by B) is considered for application to patients. The immediate effects on wellness and tumor size for the two treatments are formulated as

$$W(t_i^+ | A) = W(t_i) - 0.5, \quad M(t_i^+ | A) = 0.1M(t_i)/W(t_i), \quad (69)$$

Algorithm 2 Trajectory generation of clinical trial with a small number of treatment options

- 1: Initialize the wellness w_1 using the uniform distribution on the interval $[0.5, 1]$. Let $t_1 = 0$, $i = 1$, and the indicator of trial end $\varrho = 0$.
- 2: **while** $\varrho == 0$ **do**
- 3: Randomly choose a treatment a_i from the set $\{A, B\}$ with equal probability.
- 4: Compute the immediate effects $W(t_i^+)$ and $M(t_i^+)$ of the treatment a_i via (69) and (70).
- 5: **if** $W(t_i^+) < 0.25$ **then** ▷ The patient is dead
- 6: Let $\varrho = 1$, and $t_{i+1} = t_i$.
- 7: **else**
- 8: Draw a random number τ_i according to an exponential distribution with a mean of $0.15(W(t_i^+) + 2)/M(t_i^+)$.
- 9: Compute the critical time point \hat{t}_i via equation (73), and let $t_{i+1} = \min\{t_i + \tau_i, \hat{t}_i, 5\}$.
- 10: Compute the reward $r_i = t_{i+1} - t_i$, which represents the patient's actual survival time with the treatment a_i at the i th stage.
- 11: Compute the wellness $w_{i+1} = W(t_{i+1})$ via equation (71).
- 12: **if** $t_{i+1} == 5$ or $i == 3$ **then** ▷ The clinical trial ends
- 13: Let $\varrho = 1$.
- 14: **else** ▷ Go to the next stage
- 15: Let $i \leftarrow i + 1$.
- 16: **end if**
- 17: **end if**
- 18: **end while**

Output: i stages of trajectory data $\{w_1, a_1, r_1, \dots, w_i, a_i, r_i, w_{i+1}\}$.

$$W(t_i^+|B) = W(t_i) - 0.25, \quad M(t_i^+|B) = 0.2M(t_i)/W(t_i). \quad (70)$$

It can be seen that the aggressive treatment A yields a greater decrease in tumor size and wellness than the conservative treatment B . In the following, we rewrite both of $W(t_i^+|A)$ and $W(t_i^+|B)$ as $W(t_i^+)$, and rewrite

both of $M(t_i^+|A)$ and $M(t_i^+|B)$ as $M(t_i^+)$ for convenience. With the treatment, a patient's current survival time τ_i is drawn independently according to an exponential distribution, with a mean of $0.15(W(t_i^+) + 2)/M(t_i^+)$.

The cancer dynamics after t_i satisfy the following equations:

$$W(t) = W(t_i^+) + (1 - W(t_i^+))(1 - 2^{-(t-t_i)/2}), \quad (71)$$

$$M(t) = M(t_i^+) + 4M(t_i^+)(t - t_i)/3. \quad (72)$$

Noted that the i th stage begins at time point t_i , and ends at time point t_{i+1} such that $M(t_{i+1}) = 1$ for some $t_i < t_{i+1} < 5$, or the patient dies, or the clinical trial ends. Specifically, we can obtain the critical time point

$$\hat{t}_i = t_i + 0.75 \left(\frac{1 - M(t_i^+)}{M(t_i^+)} \right) \quad (73)$$

from $M(\hat{t}_i) = 1$, and thus compute the end of the i th stage via $t_{i+1} = \min\{\hat{t}_i, t_i + \tau_i, 5\}$.

The generation of the trajectory data is shown in Algorithm 2. We assume that only patients in urgent need of treatment are enrolled in the clinical trial, which means that all patients meet $M(0) = 1$ and thus $t_1 = 0$. The wellness of patients at the beginning of the first stage is drawn independently according to the uniform distribution in the interval $[0.5, 1]$. A treatment is randomly chosen from the set $\{A, B\}$ for each time point t_i . The reward is defined as the actual survival time of the current stage. Due to the differences in initial wellness, survival time, and treatment policies for different patients, the generated trajectories may have different numbers of stages. Here, the total number of stages for all patients is limited to 3. For the missing stages of the trajectory data with a number of stages less than 3, we fill wellness and reward as zeros and randomly choose actions from the set $\{A, B\}$ with equal probability, modifying the trajectory to a fixed length of 3.

Appendix D: Introduction of Simulation 2

This section describes the process of generating trajectory data in Section 5.2. In this simulation, patients are monitored monthly for 6 months, and a treatment is applied to each patient at the beginning of each month. The relation of a drug's toxicity W_i , tumor size M_i , and drug dosage A_i of a treatment is characterized by the following system of ordinary difference equations:

$$W_{i+1} = W_i + 0.1(M_i \vee M_0) + 1.2(A_i - 0.5), \quad (74)$$

$$M_{i+1} = (M_i + (0.15(W_i \vee W_0) - 1.2(A_i - 0.5)) \times \mathbf{1}_{M_i > 0}) \vee 0, \quad (75)$$

for $i = 1, \dots, 6$, where a month is a treatment stage, \vee is the maximum operation, and $\mathbf{1}_{M_i > 0}$ is an indicator function representing that there will be no future recurrence of the tumor when the tumor size reaches 0 (that is, the patient has been cured). The initial values of toxicity W_1 and tumor size M_1 are drawn independently according to the uniform distribution on the interval $(0, 2)$. The drug dosage treatment sets for the first and last five stages are $\{0.51, 0.52, \dots, 1\}$ and $\{0.01, 0.02, \dots, 1\}$, respectively. They are discretized from drug dosage intervals $(0.5, 1]$ and $(0, 1]$ with an increment of size 0.01. The action A_1 and the actions A_i ($i = 2, \dots, 6$) are randomly chosen from the sets $\{0.51, 0.52, \dots, 1\}$ and $\{0.01, 0.02, \dots, 1\}$ with equal probability, respectively. To increase the stochasticity of the survival status, we define the conditional probability of death for the i th stage as

$$p_i = 1 - \exp(-\exp(W_i + M_i - 4.5)). \quad (76)$$

The survival status (death is codes as 1) is drawn independently according to the Bernoulli distribution $B(p_i)$. The reward for each stage is assumed to depend on the states (including toxicity and tumor size) observed right before and after each action, and it can be decomposed into three types of rewards: $R_{i,1}(A_i, W_{i+1}, M_{i+1})$ related to survival status, $R_{i,2}(W_i, A_i, W_{i+1})$ related to toxicity change, and $R_{i,3}(M_i, A_i, M_{i+1})$ related to tumor size change. Specifically, they are defined by

$$R_{i,1}(A_i, W_{i+1}, M_{i+1}) = -6, \quad \text{if patient died,} \quad (77)$$

otherwise,

$$R_{i,2}(W_i, A_i, W_{i+1}) = \begin{cases} 0.5, & \text{if } W_{i+1} - W_i \leq -0.5, \\ -0.5, & \text{if } W_{i+1} - W_i \geq 0.5, \\ 0, & \text{if } -0.5 < W_{i+1} - W_i < 0.5, \end{cases} \quad (78)$$

$$R_{i,3}(M_i, A_i, M_{i+1}) = \begin{cases} 1.5, & \text{if } M_{i+1} = 0, \\ 0.5, & \text{if } M_{i+1} - M_i \leq -0.5 \text{ and } M_{i+1} > 0, \\ -0.5, & \text{if } M_{i+1} - M_i \geq 0.5, \\ 0, & \text{if } -0.5 < M_{i+1} - M_i < 0.5. \end{cases} \quad (79)$$

Because overall survival is the main focus of clinical interest, we take a high penalty of -6 for the death of a patient in the equation (77), and we take a relatively large bonus of 1.5 for the cure of a patient in the equation (79). In other cases, rewards are given according to the changes in toxicity and tumor size in two consecutive stages.